



**HAL**  
open science

## **GDF11 exhibits tumor suppressive properties in hepatocellular carcinoma cells by restricting clonal expansion and invasion**

Monserrat Gerardo-Ramírez, Roberto Lazzarini-Lechuga, Sharik Hernández-Rizo, Javier Esteban Jiménez-Salazar, Arturo Simoni-Nieves, Carmen García-Ruiz, José Carlos Fernández-Checa, Jens U Marquardt, Cedric Coulouarn, María Concepción Gutiérrez-Ruiz, et al.

### ► To cite this version:

Monserrat Gerardo-Ramírez, Roberto Lazzarini-Lechuga, Sharik Hernández-Rizo, Javier Esteban Jiménez-Salazar, Arturo Simoni-Nieves, et al.. GDF11 exhibits tumor suppressive properties in hepatocellular carcinoma cells by restricting clonal expansion and invasion. *Biochimica et Biophysica Acta - Molecular Basis of Disease*, 2019, 1856 (6), pp.1540-1554. 10.1016/j.bbadis.2019.03.003 . hal-02087898

**HAL Id: hal-02087898**

**<https://univ-rennes.hal.science/hal-02087898>**

Submitted on 9 Sep 2019

**HAL** is a multi-disciplinary open access archive for the deposit and dissemination of scientific research documents, whether they are published or not. The documents may come from teaching and research institutions in France or abroad, or from public or private research centers.

L'archive ouverte pluridisciplinaire **HAL**, est destinée au dépôt et à la diffusion de documents scientifiques de niveau recherche, publiés ou non, émanant des établissements d'enseignement et de recherche français ou étrangers, des laboratoires publics ou privés.

## **GDF11 exhibits tumor suppressive properties in hepatocellular carcinoma cells by restricting clonal expansion and invasion**

Montserrat Gerardo-Ramírez<sup>1,2</sup>, Roberto Lazzarini-Lechuga<sup>3</sup>, Sharik Hernández-Rizo<sup>1,2</sup>, Javier Esteban Jiménez-Salazar<sup>3</sup>, Arturo Simoni-Nieves<sup>1,2</sup>, Carmen García-Ruiz<sup>4</sup>, José Carlos Fernández-Checa<sup>4</sup>, Jens U. Marquardt<sup>5</sup>, Cedric Coulouarn<sup>6</sup>, María Concepción Gutiérrez-Ruiz<sup>2,7</sup>, Benjamín Pérez-Aguilar <sup>2,#</sup>, Luis E. Gomez-Quiroz<sup>2,7,#,\*</sup>

1. Posgrado en Biología Experimental, DCBS, Universidad Autónoma Metropolitana-Iztapalapa, Mexico City, Mexico.
2. Departamento de Ciencias de la Salud, Universidad Autónoma Metropolitana-Iztapalapa, Mexico City, Mexico.
3. Departamento de Biología de la Reproducción, Universidad Autónoma Metropolitana-Iztapalapa, Mexico City, Mexico.
4. Department of Cell Death and Proliferation, Instituto de Investigaciones Biomédicas de Barcelona, CSIC; Liver Unit, Hospital Clinic, IDIBPAS and CIBERehd, Barcelona, Spain
5. 1st Department of Medicine, University Medical Center, Johannes Gutenberg University Mainz, Langenbeckstrasse 1, 55131 Mainz, Germany
6. INSERM, Inra, University of Rennes, UMR 1241, Nutrition Metabolisms and Cancer, Rennes, France.
7. Laboratorio de Medicina Experimental, Unidad de Medicina Translacional, Instituto de Investigaciones Biomédicas, UNAM/ Instituto Nacional de Cardiología Ignacio Chavez, Mexico City, Mexico

Running title: GDF11 display antitumorigenic response in liver cancer cells

# Shared Senior authorship

\* Corresponding author. Luis E. Gomez-Quiroz, Email [legq@xanum.uam.mx](mailto:legq@xanum.uam.mx), Departamento de Ciencias de la Salud, Universidad Autónoma Metropolitana Iztapalapa. Av. San Rafael Atlixco 186, Col. Vicentina, 09340, Iztapalapa. Mexico City, Mexico. Tel/Fax: 55-58044730.

## **Abstract**

Growth differentiation factor 11 (GDF11) has been characterized as a key regulator of differentiation in cells that retain stemness features, despite some controversies in age-related studies. GDF11 has been poorly investigated in cancer, particularly in those with stemness capacity, such as hepatocellular carcinoma (HCC), one of the most aggressive cancers worldwide. Here, we focused on investigating the effects of GDF11 in liver cancer cells. GDF11 treatment significantly reduced proliferation, colony and spheroid formation in HCC cell lines. Consistently, down-regulation of CDK6, cyclin D1, cyclin A, and concomitant upregulation of p27 was observed after 24 h of treatment. Interestingly, cell viability was unchanged, but cell functionality was compromised. These effects were potentially induced by the expression of E-cadherin and Occludin, as well as Snail and N-cadherin repression, in a time-dependent manner. Furthermore, GDF11 treatment for 72 h induced that cells were incapable of sustaining colony and sphere capacity in the absence of GDF11, up to 5 days, indicating that the effect of GDF11 on self-renewal capacity is not transient. Finally, *in vivo* invasion studies revealed a significant decrease in cell migration of hepatocellular carcinoma cells treated with GDF11 associated to a decreased proliferation judged by Ki67 staining. Data show that exogenous GDF11 displays tumor suppressor properties in HCC cells.

**Keywords:** GDF11; Huh7 cells; HCC; Cell cycle; Liver cancer; Hep3B cells

## 1. Introduction

Liver diseases represent one of the main challenges in public health. Changes in human habits tend to increase the prevalence of severe liver diseases, such as steatohepatitis, cirrhosis, viral hepatitis and liver cancer [1]. Hepatocellular carcinoma (HCC) is one of the most prevalent and aggressive tumor worldwide with high rate of postsurgical recurrence [2-4], and despite the outstanding progress made in the last decade in identifying new therapeutic approaches to target canonical proliferation and survival pathways, the potential use of non-canonical molecules and the molecular basis of their anti-proliferating activity are currently being studied directed to provide new therapeutic targets [5].

Growth differentiation factor 11 (GDF11) is a member of the subfamily of the bone morphogenic proteins, and of the superfamily of the transforming growth factor beta (TGF- $\beta$ ). GDF11 is critical for organogenesis and development, particularly for skeletal system. Knock-out for mouse *Gdf11*, or for the furin-like convertase (*Pcsk5*), which activates GDF11 to a mature form, results in skeletal development defects and lethality *in utero* [6, 7].

Recently, some controversies have emerged about the effects of GDF11 in rejuvenation process [8]. While some groups report that GDF11 expression reduces with age, and its restoration induces proliferation and differentiation of progenitor cells (satellite cells) in the skeletal [9] and cardiac muscle [10], reversing the age-related hypertrophy, others state that GDF11 significantly inhibits muscle regeneration and decreases satellite cell expansion in mice [11, 12]. This debating question is also associated with the great similarity of GDF11 with myostatin (or GDF8) and the poor specificity of some commercial

antibodies [13]. Aside of these controversial functions of GDF11 in age-related disorders, both outlooks have in common that cells, with some stemness properties, are targeted by the GDF11, notably in development process [14-16]. Given that cancer cells, with stemness features, are recognized as key therapeutic target, due to their capacity of sustained proliferation and migration, possibly driving tumor progression and resistance to treatment, we aimed at figure out the effects of GDF11 in HCC-derived cell lines. Although some studies revealed that GDF11 expression correlates with poor prognosis in colorectal [17] and breast cancer [18], it has been poorly studied in this kind of disease. Recently, Bajikar and collaborators [19] reported that GDF11 exerts tumor suppressive functions in triple-negative breast cancer cells. Loss of function of GDF11 in breast cancer has been notably related to deficient maturation due to the convertase PCSK5, which activates bioactive GDF11 from its immature form. The present study is the first one related to liver cancer and provides evidence that GDF11 could be a good candidate for new therapeutic options.

## **2. Materials and Methods**

### *2.1 Cell culture*

Huh7, Hep3B, Hepa1-6, HepG2, SNU-182 and MDA-MB-231 cell lines were obtained from the American Type Culture Collection (ATCC, Manassas, VA, USA). Cells were cultured in William's medium supplemented with 10% fetal bovine serum (FBS, Hy-Clone, Logan, UT, USA), 100 U/ml ampicillin and 100 µg/ml streptomycin (Thermo Fisher Scientific, Waltham, MA, USA). Cells were maintained at 37°C in a 5% CO<sub>2</sub> and 90% humidity atmosphere. Cells were

plated in plastic culture bottles (Sigma-Aldrich, Saint Louis, MO, USA). All cell lines were mycoplasma free.

### *2.2 Main experimental design*

Cells were exposed to 50 ng/ml GDF11 [20] for different times. GDF11 was added to culture media every 24 h and cells were recovered after 72 h for experiments, as depicted in supplementary figure 1A.

In order to determine whether GDF11 effects are not transient, and remain after growth factor withdrawal, we performed additional experiments, in which cells were treated every 24 h up to 72 h, then harvested and re-plated without GDF11. Spheroid and colony formation were evaluated up to 5 days in the absent of GDF11 (Supplementary figure 1B).

### *2.3 Western blotting*

Western blot was conducted as we previously reported [21]. PVDF membranes were probed with specific antibodies as described in the supplementary table 1. Horseradish peroxidase-conjugated antibodies were used according to the primary antibodies. Blots were exposed using Super Signal West Pico Chemiluminescent substrate (Pierce Biotechnology, USA). Signal was detected using Gel Logic 2500 (Kodak, Rochester, NY, USA).

### *2.4 Immunofluorescence assays*

Immunofluorescence was conducted as previously reported [22], briefly, cells were treated for different times with GDF11, and then fixed with 4 % paraformaldehyde in phosphate-buffered saline (PBS). Samples were permeabilized with 0.01 % (v/v) Triton-X 100 for 30 min and blocked with 3 %

(w/v) bovine serum albumin (BSA) in PBS for 30 min and subsequently incubated with primary antibodies anti-occludin (Santa Cruz Biotechnology 81812, dilution 1:100), anti-snail (Santa Cruz Biotechnology 28199, dilution 1:100), anti-E-cadherin (Santa Cruz Biotechnology 21791, dilution 1:100) and anti-N-cadherin (Santa Cruz Biotechnology 59987, dilution 1:100). Nuclei were counterstained with 1 µg/mL 4',6-diamidino-2-phenylindole (DAPI) (Sigma-Aldrich). Images were obtained using a multi-photon confocal microscope (Carl Zeiss LSM-780 NLO, Oberkochen, Germany).

### *2.5 Cell proliferation*

Cell proliferation was addressed by CCK-8 kit (Dojindo Lab, Kumamoto, Japan), following manufacturer's instructions.

### *2.6 Spheroid formation*

Cells were seeded in six-well low attachment plates, (Millipore-Sigma, Saint Louis MO, USA). The cultures were supplemented every 24 h with 50 ng/ml of GDF11 for five days. The spheroids were counted and photographed using an inverted microscope Carl Zeiss VERT.A1.

### *2.7 Wound-healing assay*

Cells were seeded in six-well plates to approximately 90% of confluency. In each well a couple of wounds were created with a 20 µl pipette tip. Plates were washed three times with PBS to remove detached cells. Subsequently, media were added supplemented or not with FBS in presence or absent of GDF11.

The healing response was monitored every 24 h up to 72 h when photography register was performed.

### *2.8 Cell functionality by MTT assay*

Cell functionality was addressed by the 3-(4,5-dimethylthiazol-2-yl)-2,5-diphenyltetrazolium bromide (MTT) test, using the Vybrant MTT Cell Proliferation Assay Kit (Thermo Fisher Scientific), following manufacturer's instructions.

### *2.9 Clonogenic assay*

After 72 h under GDF11 treatment,  $1 \times 10^3$  cells were seeded into 6-well plates in triplicate and maintained in GDF11-free media, in presence or absent of FBS. After 10 days, colonies were stained with crystal violet, photographed and counted.

### *2.10 Invasion study using a chick embryo chorioallantoic membrane (CAM) assay*

Chick embryo CAM model was used to study invasion properties, following previous method reported by our group and others [23-25]. Briefly, ten fertile chick (*Gallus domesticus*) eggs (ALPES SA Farms, Puebla, Mexico) were randomly separated in two groups. Eggs were incubated at 37.8°C and 60% humidity up to 22 HH of embryo stage development. Then, shells were wiped with 70% ethanol, and 1 cm<sup>2</sup> window was done. The vitelline membrane was dissected and  $1 \times 10^6$  cells, treated or not with GDF11 for 72 h and labeled with vibrant CFDA SE cell tracer kit (Thermo Fisher Scientific), were introduced onto the CAM, in the convergence of two blood vessels, using 30  $\mu$ l of Matrigel (Sigma-Aldrich) as substrate. The window in the shells was covered with sterile

adhesive tape and eggs were incubated as above for 2 and 4 days. CAM were recovered and immediately fixed with 4% paraformaldehyde in PBS. Paraffin sections (5  $\mu$ m) were obtained for immunofluorescence using anti-beta-catenin antibody (Cell Signaling #9562). Proliferation was addressed by immunofluorescence using anti-Ki67 antibody (abcam 15580; dilution 1:100). Nuclei were counterstained with 1  $\mu$ g/ml DAPI. Images were acquired using a multi-photon confocal microscope (Carl Zeiss LSM-780 NLO).

### *2.11 Real-time quantitative reverse transcriptase-polymerase chain reaction (qRT-PCR)*

One  $\mu$ g total RNA was reverse transcribed in 20  $\mu$ l reaction volume with a SuperScript (Invitrogen Corp.) first-strand synthesis kit according to the manufacturer's instructions. Oligonucleotide primers were designed using Primer3 v.0.4.0 (<http://frodo.wi.mit.edu/primer3/>) as describe [26]. The qRT-PCR analysis was performed with a CFX96 Touch (Bio-Rad) thermal cycler in a 96-well reaction plate. The 10  $\mu$ l PCR reaction mix contained 5  $\mu$ l 2X SYBR Green PCR Master Mix (Bio-Rad), 200 nM of each primer, and 1  $\mu$ l cDNA template. Reactions were incubated for 10 min at 95°C followed by 40 cycles of 30 sec at 95°C and 60 sec at specific primer temperature. The expression level of ribosomal protein S18 (rs18) was used as reference. Relative gene expression levels were calculated using the formula  $2^{-\Delta\Delta Ct}$ . Primer sequences are listed in supplementary table 2.

### *2.12 Protein quantification*

The protein content was determined by using the bicinchoninic acid method (BCA, Pierce, Thermo Fisher Scientific.), following the manufacturer's instructions.

### *2.13 Statistical analysis*

The results are presented as the average of at least three independent experiments. A One-way ANOVA followed by Tukey post-test was performed for the analysis of cell viability, mitochondrial functionality by MTT, number of spheroids and number of colonies in cell sensitization experiments with GDF11. t-student test was performed for the analysis of the numbers of spheroids.

## **3. Results**

### *3.1 HCC cells respond to GDF11 treatment by activating Smad3*

To figure out whether HCC-derived cells respond to GDF11, Huh7 and Hep3B cells were treated with 50 ng/ml GDF11 up to 60 min. Activation of the canonical signaling pathway was addressed by immunoblot of Smad3. Figure 1A shows that Smad3 is rapidly activated by phosphorylation 5 min, in Huh7 cell line, and 30 min in Hep3B cell line, after GDF11 treatment. Activation remains up to 60 min. To explore impact in cell viability, Huh7 and Hep3B cells were treated at different times with GDF11. Time-course analysis up to 72 h of treatment demonstrates that GDF11 has no significant impact on cell viability (Figure 1B), while CdCl<sub>2</sub> (5 μM, 6 h), used as a positive control, reduces cell viability. In addition, morphology inspection of cell culture at 72 h revealed small changes in cells, including a flat-like phenotype and a decrease in cell density in both cell lines (Figure 1C).

### *3.2 GDF11 impairs cell proliferation and cycle progression*

Next, we decided to address cell proliferation; although no significant effect was observed on cell viability, GDF11 was shown to decrease Huh7 cell proliferation starting after 48 h GDF11 treatment and being statistically significantly at 72 h in the absence or presence of FBS (Figure 2A), which was used as a competitor. In addition, a wound-healing assay revealed an impaired repair process at 72 h under GDF11 treatment compared with untreated cells (Figure 2B). The analysis of the content of key cell cycle proteins shows that positive regulators such as Cyclin A, Cyclin D1 and CDK6 decreases in a time dependent manner, while CDK inhibitor p27 increases (Figure 2C). Consistent with results observed in Huh7 cells, Hep3B cells under GDF11 treatment showed similar effects in cell proliferation (Figure 2D) and wound-healing assay (Figure 2F). Although viability was not affected in both HCC-derived cell lines, cell functionality, evaluated by MTT assay was significantly decreased starting after 24 h of treatment, in Huh7 cells, and 48 h in Hep3B cells, explaining the effects observed in proliferation and wound-healing (Figure 2G).

### *3.3 GDF11 decreases spheroid formation capacity and the expression of genes related to aggressiveness*

Previous results strongly suggest that GDF11 exerts tumor suppressive effects. To gain more evidence, we performed studies of spheroid formation under GDF11 treatment every 24 h for 5 days. Cells treated with GDF11 exhibited fewer spheroids at day 5 (39%, in Huh7 cells; and 34% in Hep3B), as compared with untreated cells at the same time (Figure 3A). Even more, spheroids

observed under the GDF11 treatment were smaller (25% in Huh7 cells; and 40% in Hep3B) than those formed in the absent of treatment.

The analysis of the expression of some of the key well-characterized markers of cancer cell aggressiveness, revealed an increment of messenger RNA of CD133, CD24, CK19 and EpCAM particularly, the last one was significantly diminished only in Hep3B with no changes in Huh7 cells (Figure 3B).

#### *3.4 GDF11 promotes mesenchymal epithelial transition*

Next, we decided to address the expression of some mesenchymal and epithelial key markers in cells under GDF11 treatment. The immunoblot revealed a decrement of mesenchymal markers, such as Snail and N-cadherin, and the increment of epithelial markers, such as occludin and E-cadherin, in a time-dependent manner (Figure 4A and B), interestingly mesenchymal markers remain below levels of not treated cells, while epithelial markers decrement peaked at 24 h and then decreased to control values. To gain more confidence of these data, we analyzed the content of these proteins by immunofluorescence, figure 4C and D show the colocalization of Snail and E-cadherin; and N-cadherin and Occludin, respectively, in both cases the expression of the mesenchymal proteins (Snail or N-cadherin) was considerably diminished, and the epithelial ones was increased, confirming the immunoblot experiments. Similar results were obtained in Hep3B exhibiting an increment in the expression of E-cadherin and occludin, and decrement in N-cadherin, in a time-dependent manner (Supplementary figure 2)

### *3.5 The effects elicited by GDF11 for 72 h of treatment remain in the absence of the factor.*

To figure out whether the effects displayed by GDF11 induce a long-lasting or a transient cellular reprogramming, cells were treated with GDF11 every 24 h for three days then, cells were harvested and processed to explore the capacity of colony and spheroid formation for five days, in presence or absence of serum as competitor. Figure 5A shown that Huh7 cells treated with GDF11 remarkably decreased the ability to form colonies, in the presence or absence of FBS. Similarly, spheroid formation was significantly diminished in both cell lines (Figure 5 B and C), interestingly a better effect was observed in Huh7 cell line practically abrogating the spheroid formation capacity. Serum supplementation in the media did not rescue cells from the static phenotype (Supplementary figure 3), but the number of spheroids were different in the presence or absent of FBS in NT cells. Reprogramming experiments showed that cells exposed to GDF11 were unable of sustaining their colony and sphere forming capacity, indicating that the effect of GDF11 on self-renewal capacity is not transient.

### *3.6 GDF11 impairs invasion capacity*

To address one of the key hallmarks of malignancy, we assayed invasion property in cells treated or not with GDF11.  $1 \times 10^6$  cells were grafted in the CAM of the chick embryo (Figure 6A). Figure 6C shows the complete control CAM with no cells, in order to observe normal morphology of the CAM. Cells were grafted in the area labeled with the yellow circle; the eggshell was covered with sterile tape. After two or four days of incubation at 37 °C, the CAM was recovered fixed and paraffin embedded for immunofluorescence and confocal

microscopy. We started exploring the effect at day four; at this time we observed embryo lethality only with not treated cells (Figure 6B). Microscopy inspection revealed few disaggregated not treated cells remaining in the grafted zone (Supplementary figure 4A, white arrows), and some cells were observed in the distal zone of the CAM (green cells), indicating an ongoing invasion process (Supplementary figure 4C). The same experimental setting with GDF11 treated cells revealed some significant compacted aggregates of cells (Supplementary figure 4B, yellow arrow heads), and some of them in transit (Supplementary figure 4B, white arrows). No cell was detected in the distal CAM (Supplementary figure 4D). Remarkably, chick embryos in the eggs inoculated with GDF11 treated cells were still alive (Figure 6B).

In order to analyze the invasion process at an early time point, we decided to incubate the eggs only for two days. Microscopic analysis of the complete CAM revealed that most of the untreated cells were gone (Figure 6D). In fact, some of chick embryo dies also at this time, however, cells treated for three days with GDF11 remained covered by the CAM and cell localization suggests an attempt of migration, but most of the cells still there (Figure 6E). The CAM zones near to the cell cumulous strongly express beta catenin (yellow arrow, and figure inset), probably as a response to Huh7 cells reprogramming induced by GDF11; in comparison, beta catenin expression in CAM with non-treated cells, was weak, suggesting degradation. In order to address the cell proliferation status in the invasion experiment, we proceeded to detect Ki67 protein content by immunofluorescence; figure 6F shows more proliferating cells in CAM grafted with not treated Huh7 cells comparing with those under GDF11 treatment;

remarkably, Ki67 positive cells were more abundant in the lower zone of the CAM, indicating more proliferative capacity (yellow arrow; Figure 6F).

To corroborate the GDF11-induced invasion restriction, we performed the CAM experiment using Hep3B cells. The results depicted in supplementary figure 3E show disaggregated not treated cells in the engraftment zone, cells seem to be disabled to form cell to cell interactions, in comparison with GDF11 treated cells that exhibited a well compacted cell cumulus with well defined cell interactions, the vascular zone exhibited not treated cells in blood vessels, effect that was absent in GDF11-treated cells, interestingly, the tumor was well delimited (white arrows, supplementary figure 4), suggesting that treated cells were able to degrade the basal membrane, as observed in an *in situ* tumor. The distal zone in the experiment with not treated cells shows many disaggregated cells in the CAM, in comparison of the GDF11 experiment with few cells; remarkably, the size of this zone was thicker than that with not treated cells. Thus, these data strongly suggest that GDF11 significantly reduces invasive property.

### *3.7 GDF11 decreases spheroid formation in other cancer cell lines.*

Finally, to corroborate that the tumor suppressive effects displayed by GDF11 are not restricted to Huh7 and Hep3B cell line, we treated for three days the human hepatoma cell line HepG2 (Figure 7A), the mouse HCC cell line Hepa1-6 (Figure 7B), the human breast cancer cell line MDA-231 (Figure 7C), and the human HCC cell line SNU-182. In all cases, GDF11 significantly decreases spheroid-forming capacity, suggesting a conserved effect among cancer cells with some stemness phenotype.

#### 4. Discussion

HCC accounts for 90% of primary liver cancer, with increasing new cases every year, raising a warning worldwide [4, 27]. Although, some therapeutic options are currently well established, such as sorafenib administration for advanced tumors, local ablation or resection, these options only provide some limited benefits in terms of patient survival. Besides, liver transplantation remains a great challenge due to the limited number of donors.

Investigation of signaling pathways involved in the control of proliferation, survival or the metabolism of cancer cells is crucial to define novel alternative therapeutic approaches.

GDF11, a relatively new member of the TGF- $\beta$  superfamily, has been showed to display biological effects in a wide range of cell types. It is particularly interesting that most of the cells that respond to GDF11 exhibit some degree of stemness phenotype [9, 20]. Along this characteristic, we hypothesized that this growth factor could exert some effects in HCC-derived cell lines, particularly in those retaining stemness features. It was reported that Huh7 cell line expresses some of the key stemness markers, such as Nanog, Oct4 or Sox2. It has been also reported that increased expression of these genes in Huh7 cells is related to the increment of stemness [28, 29], particularly when cells are forming spheroids [30]. The first evidence that Huh7 and Hep3B cells respond to GDF11 was the activation of one of the canonical signal transducers, specifically the phosphorylation of Smad3 [11, 20], which was strongly detected after 5 min of GDF11 treatment in the case of Huh7 and, at 30 min in Hep3B cells, and remained activated along 60 min (Figure 1A). It is well-characterized

that some members of the TGF- $\beta$  display effects in epithelial cells that modulate survival or proliferation [31]. Interestingly, we found that viability is unaffected up to 72 h under GDF11 treatment (Figure 1B), with no outward changes in cell phenotype. However, cell proliferation is clearly diminished at 72 h, in presence or not, of the proliferative action of FBS (Figure 2A and D), suggesting cytostatic effects similar to those observed with other members of the TGF- $\beta$  family. Indeed, it is reported that TGF- $\beta$  by itself, displays cytostatic and apoptotic functions that restrain cell growth, avoiding the hyperproliferative disorders, even in Huh7 and Hep3B cells [32, 33]. This novel effect, elicited by GDF11 in liver cancer cells, confirms the well-conserved cytostatic effect in the TGF- $\beta$  family, as exemplified by the analysis of the content of the main cell cycle regulating proteins; cyclins A and D1, and cdk6 were downregulated, and p27 was overexpressed, these effects being particularly evident at 72 h (Figure 2C). Similarly, GDF11 significantly attenuated the proliferation of the neural stem cell line Cor-1, downregulating key positive cell cycle proteins [20]. In addition, this work by Williams and collaborators showed that cell migration is impaired by GDF11 as we also observed (Figure 2B and F).

Based in the fact that stemness feature is increasing in spheroid or 3D culture, particularly in cells used in this study [29, 30], we observed that the number and the size of spheroids decreased in the presence of GDF11 at 72 h of repeated treatment (50 ng/ml, every 24 h) in both HCC cell lines. We found similar effects in HepG2 (Figure 7A), a human hepatoma cell line capable to form spheroids as well [30], and in SNU-182, another human HCC cell line from a high aggressive tumor. Interestingly, when comparing the human liver cancer cell lines, GDF11 displayed greater effects in Huh7 and Hep3B than in HepG2, although, in the

last one, decrement in sphere formation was statistically significant, confirming the preference of GDF11 on cells with stemness feature. Similar results were reported by Bajikar and collaborators in triple negative breast cancer cell lines [19], even more, Hepa1-6, MDA-MB-231 and SNU-182 cell lines presented similar effects with some differences in the number of spheroids, but in all cases with significant changes (Figure 7).

To gain more evidence, we performed the analysis of the messenger RNA levels of key molecular markers for aggressive cancers and stemness (Figure 3B), cytokeratin 19 (ck19) has been closely related to poor prognosis and high recurrence in HCC [34], the effect on ck19 expression, induced by GDF11, was the most relevant, in terms of absolute values comparing with NT cells, prom1 (CD133) and epcam (EpCAM) also are well characterized stemness markers, being CD133 most significant in stages I, while the prognostic role of EpCAM is more effective in advanced stages [35], interestingly, the effect of GDF11 in epcam expression was different in the HCC cell lines studied here, Huh7 cells did not respond to the GDF11 treatment exhibiting no changes in the expression, however, Hep3B, which a more aggressive cell line, diminished the expression since 6 h of treatment, supporting the findings by Chang and coworkers [35]. These results strongly suggest that GDF11 antitumorigenic properties are more relevant in advanced tumors. Finally, cd24 is another well-known marker for stemness and aggressive HCC [36], our data clearly show a decrement since 6 h in Huh7 and at 12 h in Hep3B, once again the difference in stemness capacity is evident in both cell lines, but in both cases GDF11 displays antitumorigenic effects.

The analysis of mesenchymal and epithelial markers revealed a clear GDF11-induced mesenchymal to epithelial transition phenotype. A time-dependent decrement in the expression of mesenchymal-related proteins such as Snail and N-cadherin, and increased of epithelial markers, such as E-cadherin and Occludin (Figure 4) [37], was confirmed by Western blot and immunofluorescence. The gain of an epithelial phenotype was simultaneously associated to a significant decrease in colony and spheroid formation capacity (Figure 5), and to a decreased capacity in invasion (Figure 6), as addressed by the CAM assay. Interestingly, in the CAM assay we observed a degradation of the basal membrane, a key condition for invasion in the experiment using not treated cells, and in the case of the experiment with GDF11 treated cells the membrane was preserved suggesting a distinctive phenotype of an *in situ* tumor, in addition treated cells were presented forming cumulous, probably because the increment of E-cadherin expression (Figure 4 and supplementary figure 2).

All these data clearly show that GDF11 induces an anti-tumor response in HCC cells, directed to decreases aggressiveness by attempting reverse the mesenchymal to epithelial phenotype.

The decrement of the invasive phenotype was also found in triple negative breast cancer cell lines [19]. The effect was associated to an increase in the expression of E-cadherin, supporting our findings in HCC-derived cells. Importantly, we reported that GDF11 effects were not transient, and may evoke a cellular reprogramming in HCC cells. Indeed, treatment for 72 h with GDF11 sustained the effects even five days in culture in the absent of GDF11.

Although, a low frequency of mutations in GDF11 and a significant enrichment in the convertase PCSK5 locus have been reported in breast cancer [19], we did not find significant presence of mutations in those genes in HCC according to The Cancer Genome Atlas (TCGA, data not shown). However, in human HCC the expression level of GDF11 observed no changes, but in cholangiocellular carcinoma (CCC), significant differences were found increasing 1.55-fold change in tumors versus normal tissue (Supplementary figure 5), (36 patients for CCC and 371 for HCC; <https://portal.gdc.cancer.gov> and <http://firebrowse.org>), in the case of PCSK5 gene expression the TCGA reports significant changes in both HCC and CCC (1.56-fold and 2.31-fold change versus normal tissue).

These data suggest that changes in basal expression in GDF11 and PCSK5 genes, are rare events in HCC and probably not responsible to the loss of function of GDF11, maybe some epigenetic silencing mechanism could be related to loss of function of GDF11. Nevertheless, we clearly demonstrated that recombinant human GDF11 induces an antitumorigenic effect with no relevance in cell death, but lessening aggressiveness by promoting a cytostatic phenotype and repressing invasion.

In conclusion, we are reporting tumor suppressive properties of GDF11 in HCC-derived cells restricting self-renewal capacity, setting GDF11 as a good candidate for therapy and biomarker in liver cancer.

### **Conflicts of interest**

The authors declare no conflict of interest.

### **Acknowledgements**

This work was partially funded by a grant from the Consejo Nacional de Ciencia y Tecnología (CONACYT; CB-252942 and Fronteras de la Ciencia-1320) and Universidad Autónoma Metropolitana. We thank the confocal core units of the Universidad Autónoma Metropolitana Iztapalapa, and Instituto Nacional de Cancerología de México, for the assistance. MGR, SHR, ASN are scholarship holders from Conacyt.

## References

- [1] N. Mendez-Sanchez, E. Garcia-Villegas, B. Merino-Zeferino, S. Ochoa-Cruz, A.R. Villa, H. Madrigal, R.A. Kobashi-Margain, Y. Gutierrez-Grobe, N. Chavez-Tapia, G. Ponciano-Rodriguez, M. Uribe, Liver diseases in Mexico and their associated mortality trends from 2000 to 2007: A retrospective study of the nation and the federal states, *Annals of hepatology*, 9 (2010) 428-438.
- [2] A. Forner, J.M. Llovet, J. Bruix, Hepatocellular carcinoma, *Lancet*, 379 (2012) 1245-1255.
- [3] P. Kaposi-Novak, J.S. Lee, L. Gomez-Quiroz, C. Coulouarn, V.M. Factor, S.S. Thorgeirsson, Met-regulated expression signature defines a subset of human hepatocellular carcinomas with poor prognosis and aggressive phenotype, *The Journal of clinical investigation*, 116 (2006) 1582-1595.
- [4] J. Ferlay, I. Soerjomataram, R. Dikshit, S. Eser, C. Mathers, M. Rebelo, D.M. Parkin, D. Forman, F. Bray, Cancer incidence and mortality worldwide: sources, methods and major patterns in GLOBOCAN 2012, *Int J Cancer*, 136 (2015) E359-386.

- [5] J. Bruix, M. Colombo, Hepatocellular carcinoma: current state of the art in diagnosis and treatment, *Best practice & research. Clinical gastroenterology*, 28 (2014) 751.
- [6] A.C. McPherron, A.M. Lawler, S.J. Lee, Regulation of anterior/posterior patterning of the axial skeleton by growth/differentiation factor 11, *Nat Genet*, 22 (1999) 260-264.
- [7] R. Essalmani, A. Zaid, J. Marcinkiewicz, A. Chamberland, A. Pasquato, N.G. Seidah, A. Prat, In vivo functions of the proprotein convertase PC5/6 during mouse development: Gdf11 is a likely substrate, *Proc Natl Acad Sci U S A*, 105 (2008) 5750-5755.
- [8] C.E. Brun, M.A. Rudnicki, GDF11 and the Mythical Fountain of Youth, *Cell Metab*, 22 (2015) 54-56.
- [9] M. Sinha, Y.C. Jang, J. Oh, D. Khong, E.Y. Wu, R. Manohar, C. Miller, S.G. Regalado, F.S. Loffredo, J.R. Pancoast, M.F. Hirshman, J. Lebowitz, J.L. Shadrach, M. Cerletti, M.J. Kim, T. Serwold, L.J. Goodyear, B. Rosner, R.T. Lee, A.J. Wagers, Restoring systemic GDF11 levels reverses age-related dysfunction in mouse skeletal muscle, *Science*, 344 (2014) 649-652.
- [10] F.S. Loffredo, M.L. Steinhauser, S.M. Jay, J. Gannon, J.R. Pancoast, P. Yalamanchi, M. Sinha, C. Dall'Osso, D. Khong, J.L. Shadrach, C.M. Miller, B.S. Singer, A. Stewart, N. Psychogios, R.E. Gerszten, A.J. Hartigan, M.J. Kim, T. Serwold, A.J. Wagers, R.T. Lee, Growth differentiation factor 11 is a circulating factor that reverses age-related cardiac hypertrophy, *Cell*, 153 (2013) 828-839.
- [11] M.A. Egerman, S.M. Cadena, J.A. Gilbert, A. Meyer, H.N. Nelson, S.E. Swalley, C. Mallozzi, C. Jacobi, L.L. Jennings, I. Clay, G. Laurent, S. Ma, S. Brachat, E. Lach-Trifilieff, T. Shavlakadze, A.U. Trendelenburg, A.S. Brack, D.J.

Glass, GDF11 Increases with Age and Inhibits Skeletal Muscle Regeneration, *Cell Metab*, 22 (2015) 164-174.

[12] D.J. Glass, Elevated GDF11 Is a Risk Factor for Age-Related Frailty and Disease in Humans, *Cell Metab*, 24 (2016) 7-8.

[13] M.J. Schafer, E.J. Atkinson, P.M. Vanderboom, B. Kotajarvi, T.A. White, M.M. Moore, C.J. Bruce, K.L. Greason, R.M. Suri, S. Khosla, J.D. Miller, H.R. Bergen, 3rd, N.K. LeBrasseur, Quantification of GDF11 and Myostatin in Human Aging and Cardiovascular Disease, *Cell Metab*, 23 (2016) 1207-1215.

[14] G. Finkenzeller, G.B. Stark, S. Strassburg, Growth differentiation factor 11 supports migration and sprouting of endothelial progenitor cells, *J Surg Res*, 198 (2015) 50-56.

[15] F. Jeanplong, S.J. Falconer, J.M. Oldham, N.J. Maqbool, M. Thomas, A. Hennebry, C.D. McMahon, Identification and expression of a novel transcript of the growth and differentiation factor-11 gene, *Mol Cell Biochem*, 390 (2014) 9-18.

[16] K.K. Gokoffski, H.H. Wu, C.L. Beites, J. Kim, E.J. Kim, M.M. Matzuk, J.E. Johnson, A.D. Lander, A.L. Calof, Activin and GDF11 collaborate in feedback control of neuroepithelial stem cell proliferation and fate, *Development*, 138 (2011) 4131-4142.

[17] T. Yokoe, T. Ohmachi, H. Inoue, K. Mimori, F. Tanaka, M. Kusunoki, M. Mori, Clinical significance of growth differentiation factor 11 in colorectal cancer, *Int J Oncol*, 31 (2007) 1097-1101.

[18] C. Wallner, M. Drysch, M. Becerikli, H. Jaurich, J.M. Wagner, S. Dittfeld, J. Nagler, K. Harati, M. Dadras, S. Philippou, M. Lehnhardt, B. Behr, Interaction

with the GDF8/11 pathway reveals treatment options for adenocarcinoma of the breast, *Breast*, 37 (2018) 134-141.

[19] S.S. Bajikar, C.C. Wang, M.A. Borten, E.J. Pereira, K.A. Atkins, K.A. Janes, Tumor-Suppressor Inactivation of GDF11 Occurs by Precursor Sequestration in Triple-Negative Breast Cancer, *Dev Cell*, 43 (2017) 418-435 e413.

[20] G. Williams, M.P. Zentar, S. Gajendra, M. Sonogo, P. Doherty, G. Lalli, Transcriptional basis for the inhibition of neural stem cell proliferation and migration by the TGFbeta-family member GDF11, *PLoS One*, 8 (2013) e78478.

[21] C. Enriquez-Cortina, M. Almonte-Becerril, D. Clavijo-Cornejo, M. Palestino-Dominguez, O. Bello-Monroy, N. Nuno, A. Lopez, L. Bucio, V. Souza, R. Hernandez-Pando, L. Munoz, M.C. Gutierrez-Ruiz, L.E. Gomez-Quiroz, Hepatocyte growth factor protects against isoniazid/rifampicin-induced oxidative liver damage, *Toxicological sciences : an official journal of the Society of Toxicology*, 135 (2013) 26-36.

[22] J.U. Marquardt, D. Seo, L.E. Gomez-Quiroz, K. Uchida, M.C. Gillen, M. Kitade, P. Kaposi-Novak, E.A. Conner, V.M. Factor, S.S. Thorgeirsson, Loss of c-Met accelerates development of liver fibrosis in response to CCl(4) exposure through deregulation of multiple molecular pathways, *Biochim Biophys Acta*, 1822 (2012) 942-951.

[23] J.P. Quigley, P.B. Armstrong, Tumor cell intravasation elucidated: the chick embryo opens the window, *Cell*, 94 (1998) 281-284.

[24] D. Ribatti, The chick embryo chorioallantoic membrane (CAM) assay, *Reprod Toxicol*, 70 (2017) 97-101.

- [25] R. Lazzarini-Lechuga, O. Alcantar-Ramirez, R. Jaime-Cruz, L. Gómez-Quiroz, Efecto teratogénico de nanopartículas de oro de 20 nm durante la septación cardiaca. , *Munod Nano*, 7 (2014) 69-77.
- [26] C. Czuderna, M. Palestino-Dominguez, D. Castven, D. Becker, L. Zanon-Rodriguez, J. Hajduk, F.L. Mahn, M. Herr, D. Strand, S. Strand, S. Heilmann-Heimbach, L.E. Gomez-Quiroz, M.A. Worns, P.R. Galle, J.U. Marquardt, Ginkgo biloba induces different gene expression signatures and oncogenic pathways in malignant and non-malignant cells of the liver, *PLoS One*, 13 (2018) e0209067.
- [27] A. Jemal, E.M. Ward, C.J. Johnson, K.A. Cronin, J. Ma, B. Ryerson, A. Mariotto, A.J. Lake, R. Wilson, R.L. Sherman, R.N. Anderson, S.J. Henley, B.A. Kohler, L. Penberthy, E.J. Feuer, H.K. Weir, Annual Report to the Nation on the Status of Cancer, 1975-2014, Featuring Survival, *J Natl Cancer Inst*, 109 (2017).
- [28] L. Ghisolfi, A.C. Keates, X. Hu, D.K. Lee, C.J. Li, Ionizing radiation induces stemness in cancer cells, *PLoS One*, 7 (2012) e43628.
- [29] H. Hirschfield, C.B. Bian, T. Higashi, S. Nakagawa, T.Z. Zeleke, V.D. Nair, B.C. Fuchs, Y. Hoshida, In vitro modeling of hepatocellular carcinoma molecular subtypes for anti-cancer drug assessment, *Exp Mol Med*, 50 (2018) e419.
- [30] H.S. Seol, S.E. Lee, J.S. Song, J.K. Rhee, S.R. Singh, S. Chang, S.J. Jang, Complement proteins C7 and CFH control the stemness of liver cancer cells via LSF-1, *Cancer Lett*, 372 (2016) 24-35.
- [31] Y. Zhang, P.B. Alexander, X.F. Wang, TGF-beta Family Signaling in the Control of Cell Proliferation and Survival, *Cold Spring Harb Perspect Biol*, 9 (2017).

- [32] P.M. Siegel, J. Massague, Cytostatic and apoptotic actions of TGF-beta in homeostasis and cancer, *Nat Rev Cancer*, 3 (2003) 807-821.
- [33] J. Zhang, O. Yamada, S. Kida, Y. Matsushita, T. Hattori, Down-regulation of osteopontin mediates a novel mechanism underlying the cytostatic activity of TGF-beta, *Cell Oncol (Dordr)*, 39 (2016) 119-128.
- [34] C.W. Lee, S.E. Lin, H.I. Tsai, P.J. Su, C.H. Hsieh, Y.C. Kuo, C.M. Sung, C.Y. Lin, C.N. Tsai, M.C. Yu, Cadherin 17 is related to recurrence and poor prognosis of cytokeratin 19-positive hepatocellular carcinoma, *Oncol Lett*, 15 (2018) 559-567.
- [35] A.W. Chan, J.H. Tong, S.L. Chan, P.B. Lai, K.F. To, Expression of stemness markers (CD133 and EpCAM) in prognostication of hepatocellular carcinoma, *Histopathology*, 64 (2014) 935-950.
- [36] Y. Li, R. Wang, S. Xiong, X. Wang, Z. Zhao, S. Bai, Y. Wang, Y. Zhao, B. Cheng, Cancer-associated fibroblasts promote the stemness of CD24(+) liver cells via paracrine signaling, *J Mol Med (Berl)*, 97 (2019) 243-255.
- [37] W. Chengye, T. Yu, S. Ping, S. Deguang, W. Keyun, W. Yan, Z. Rixin, L. Rui, G. Zhenming, Y. Mingliang, W. Liming, Metformin reverses bFGF-induced epithelial-mesenchymal transition in HCC cells, *Oncotarget*, 8 (2017) 104247-104257.

### Figure legends

**Figure 1. HCC cells respond to GDF11 treatment activating Smad3 with no effects on cell viability.** Huh7 and Hep3B cells were treated for different times with GDF11 (50 ng/ml). A) Western blot analysis of the Smad3 phosphorylation. Actin was used as loading control. B) Time-course analysis of cell viability

determined by crystal violet staining, cadmium chloride ( $\text{Cl}_2\text{Cd}$ ,  $5\mu\text{M}$  for 6h) was used as positive control (PC). Each column represents the mean  $\pm$  SEM of at least four independent experiments carried out by triplicate. C) Cell morphology under GDF11 treatment at 72 h, cells were treated every 24 h with GDF11 up to 72 h. Representative images of at least four independent experiments. Original magnification 200X.

**Figure 2. GDF11 impairs proliferation, migration and cellular function.** A) Huh7 cell proliferation addressed by CCK-8 in the absent or the presence of fetal bovine serum (FBS). B) Wound-healing assay, Huh7 cells were treated every 24 h with GDF11 up to 72 h. Representative images of at least four independent experiments. C) Western blot of the main cell cycle proteins and densitometric analysis. D) Hep3B cell proliferation addressed by CCK-8 in the absent or the presence of FBS. Each point represents the mean  $\pm$  SEM of at least four independent experiments carried out by triplicate, F) Wound-healing assay, Hep3B cells were treated every 24 h with GDF11 up to 72 h. Representative images of at least four independent experiments. G) Mitochondrial functionality by MTT assay in HCC cell lines, each column represents the mean  $\pm$  SEM of at least three independent experiments carried out by triplicate. Images are representative of at least three independent experiments. \*,  $p \leq 0.05$  vs NT cells at 72 h.

**Figure 3. GDF11 decreases spheroid formation capacity and the expression of genes related to aggressiveness.** A) Spheroid counting at 72 h, Huh7 and Hep3B cells were treated every 24 h with GDF11 (50 ng/ml) up to

72 h, each point represents an independent experiment, we reported the median  $\pm$  SEM of at least ten independent experiments. Images are representative of at least ten independent experiments, original magnification 100X.  $\&$ ,  $p \leq 0.05$  vs NT cells at 72 h. B) Messenger RNA levels of key genes related to cancer aggressiveness, relative expression to not treated (NT) cells is demonstrated as means  $\pm$  SEM. \*,  $p \leq 0.05$  vs NT cells.

**Figure 4. GDF11 promotes mesenchymal to epithelial transition.** A) Time-course analysis by Western blot of representative epithelial (E-cadherin and occludin) and mesenchymal (Snail and N-cadherin) markers in Huh7 cells treated with GDF11 (50 ng/ml) and, B) corresponding densitometric analysis. Each column represents the mean  $\pm$  SEM of at least three independent experiments carried out by triplicate. Images are representative of at least three independent experiments. \*,  $p \leq 0.05$  vs NT cells. Immunofluorescence determined by confocal microscopy of C) Snail and E-cadherin content and, D) N-cadherin and Occludin content. Images are representative of at least three independent experiments. Original magnification 360X.

**Figure 5. The effects elicited by GDF11 remains in the absent of the growth factor.** Cells were treated every 24 h with GDF11 (50 ng/ml) up to 72h, after that, cells were harvested and we proceeded to analyze: A) colony formation and, B) spheroid formation with deprivation of GDF11. Experiments were conducted in the presence or absence of fetal bovine serum (FBS). For the number of colonies each column represents the mean  $\pm$  SEM of at least three independent experiments carried out by triplicate. Representative images

of the six-well plates. For spheroid formation, each point represents an independent experiment; we reported the median  $\pm$  SEM of at least nine independent experiments. \*,  $p \leq 0.05$  vs NT cells in presence of FBS (+FBS); &,  $p \leq 0.05$  vs NT cells in the absence of FBS (-FBS).

**Figure 6. GDF11 impairs invasive capacity.** The chick embryo chorioallantoic membrane (CAM) model was used to address the invasion capacity as specified in Material and Methods.  $1 \times 10^6$  cells treated or not with GDF11 for 72 h, were engrafted in the top of the CAM in 30  $\mu$ l of Matrigel. A) Schematic representation of the model used in the study. B) Survival plot of the chicken embryo,  $n=6$  in each treatment. C) Representative confocal image composition of the control complete CAM, the yellow circle indicates the place where cells were placed. D) Confocal microscopic inspection of the entire CAM that received not treated Huh7 cells. E) Confocal microscopic inspection of the entire CAM that received GDF11 treated Huh7 cells for 72 h. CAM is identified by immunofluorescence of beta catenin (membrane in green, yellow arrows), DAPI was used for nuclei identification, Huh7 cells were traced with Vybrant CFDA SE cell tracer kit (white arrows). F) Ki67 immunofluorescence, positive cells in green (Alexa flour 488), nuclei in red (propidium iodide). V, blood vessel. Images are representative of at least 6 eggs per condition.

**Figure 7. GDF11 decreases spheroid formation property in other cancer cell lines.** Cells were treated every 24h with GDF11 (50 ng/ml) up to 72 h and we proceeded to spheroid counting in A) HepG2, hepatoblastoma cell line B) Hepa1-6, mouse hepatocellular carcinoma cell line, C) MDA-MB-231, triple

negative breast cancer cell line, D) SNU-182, grade III/IV human hepatocellular carcinoma cell line. Each point represents an independent experiment; we reported the median  $\pm$  SEM of at least six independent experiments. \*,  $p \leq 0.05$  vs NT cells at 72 h.

Accepted manuscript

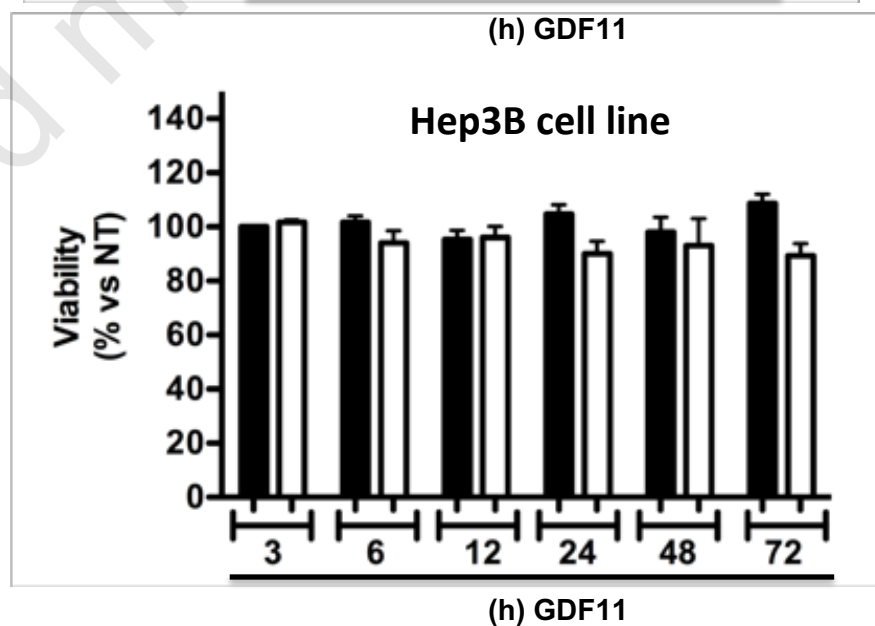
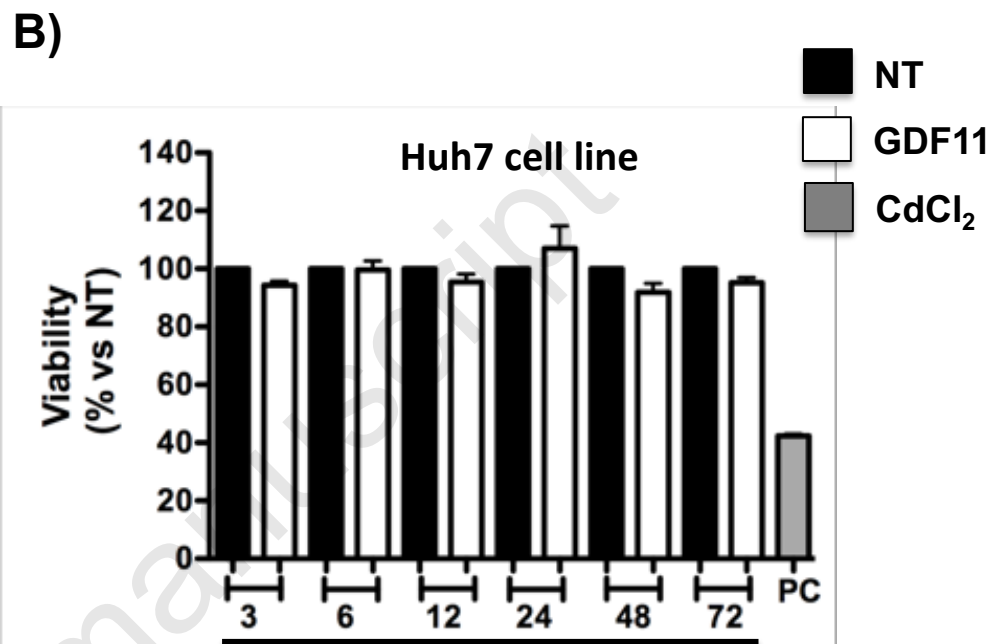
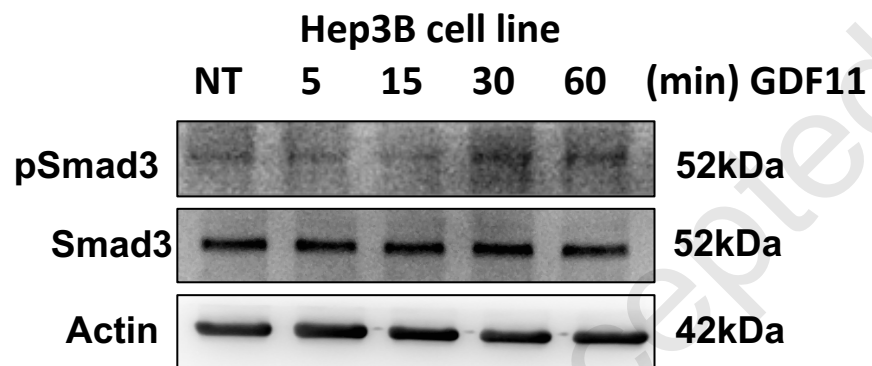
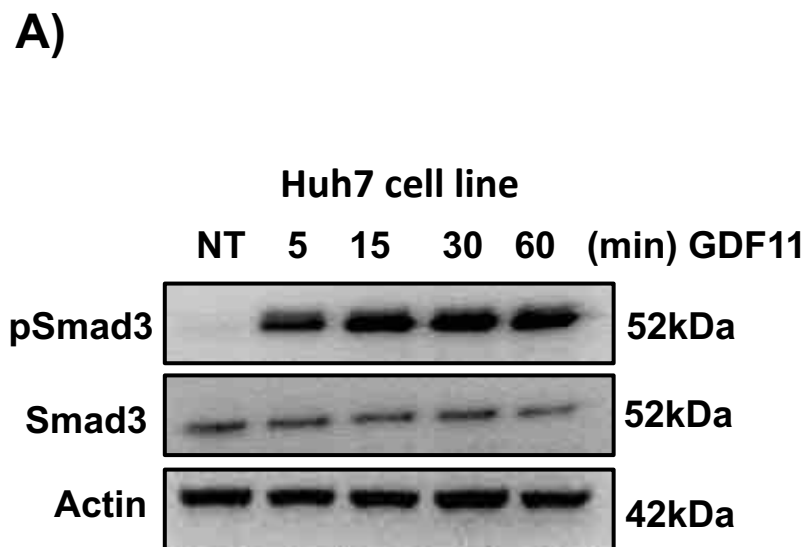


**Figure 1**

**Figure 1**

**C)**

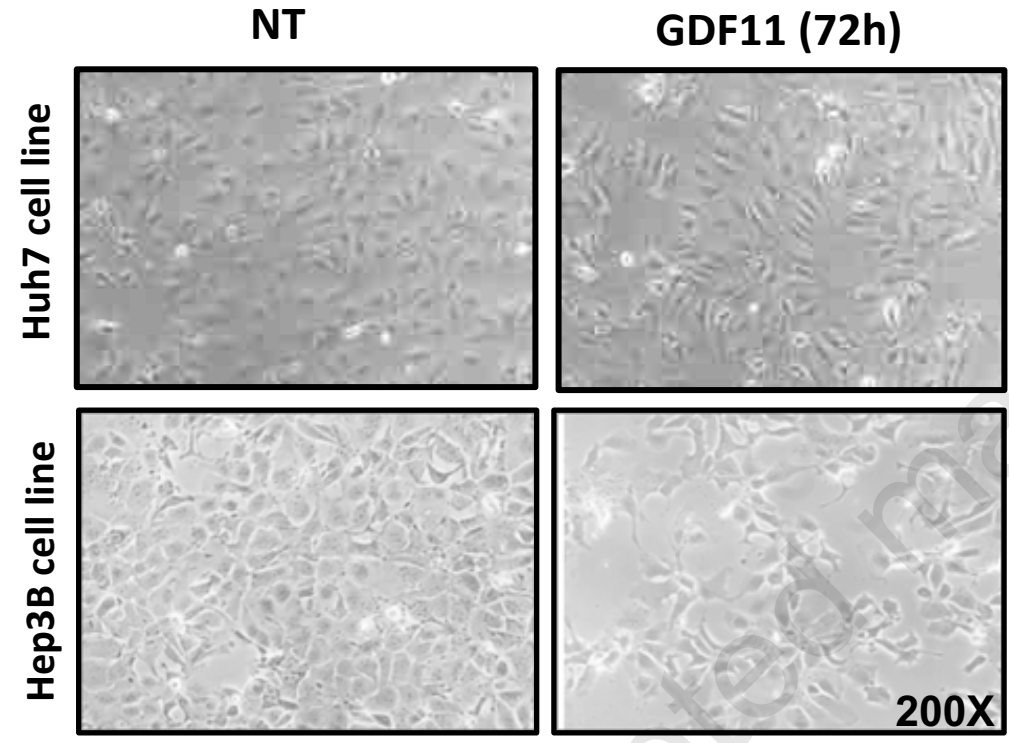
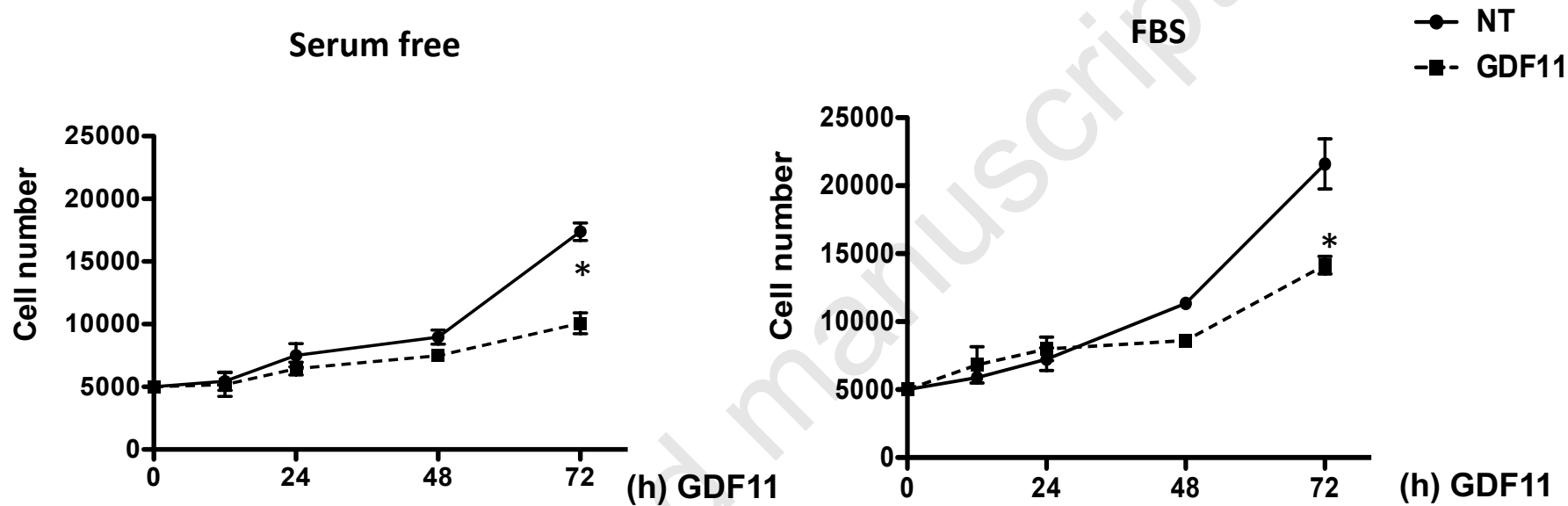


Figure 2

A)



B)

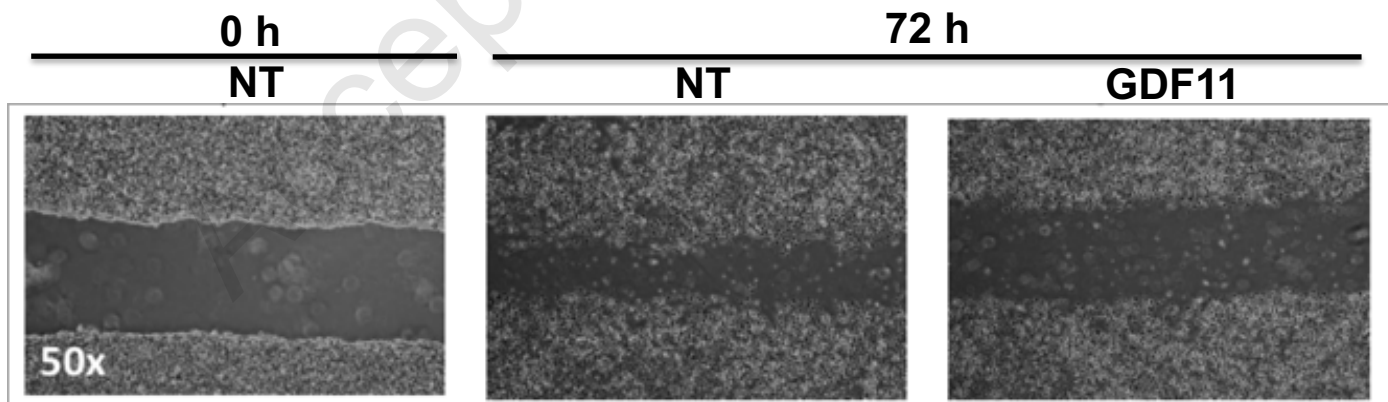
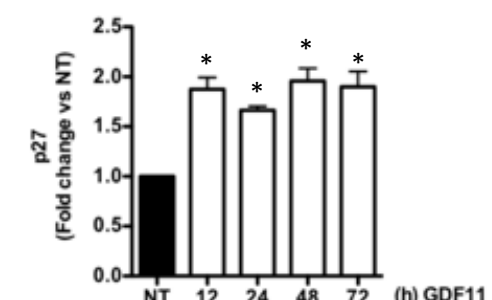
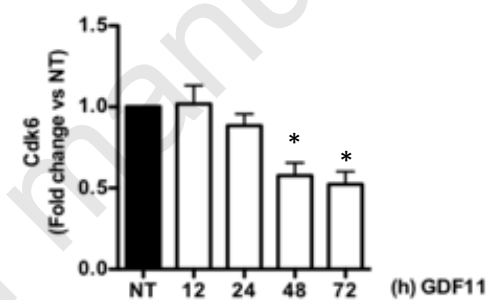
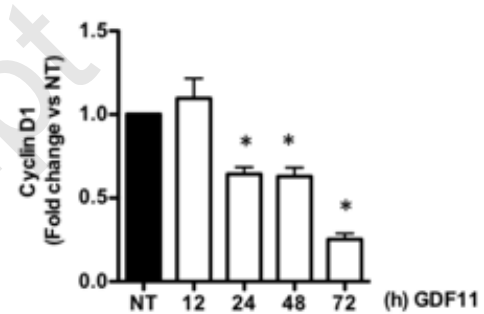
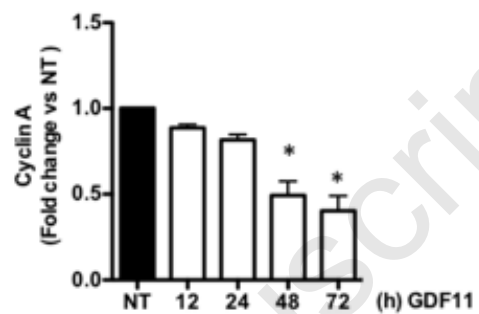
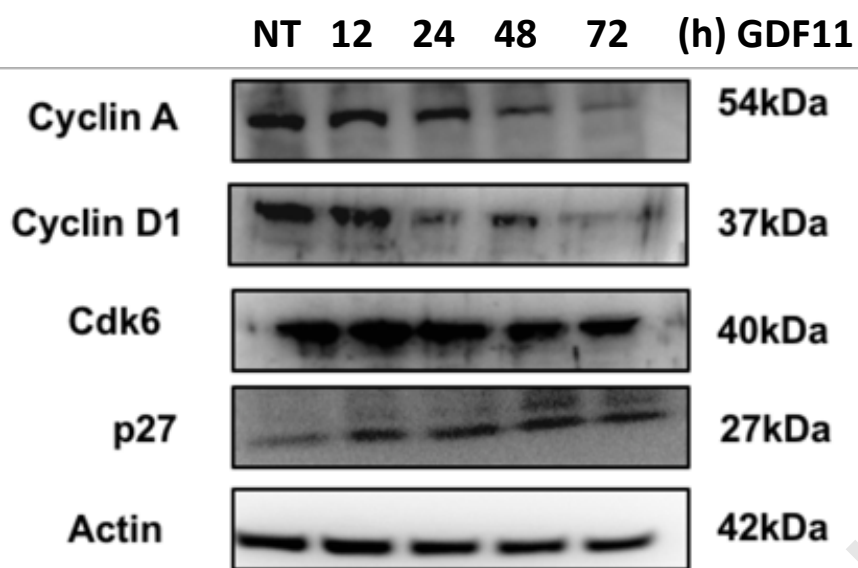


Figure 2

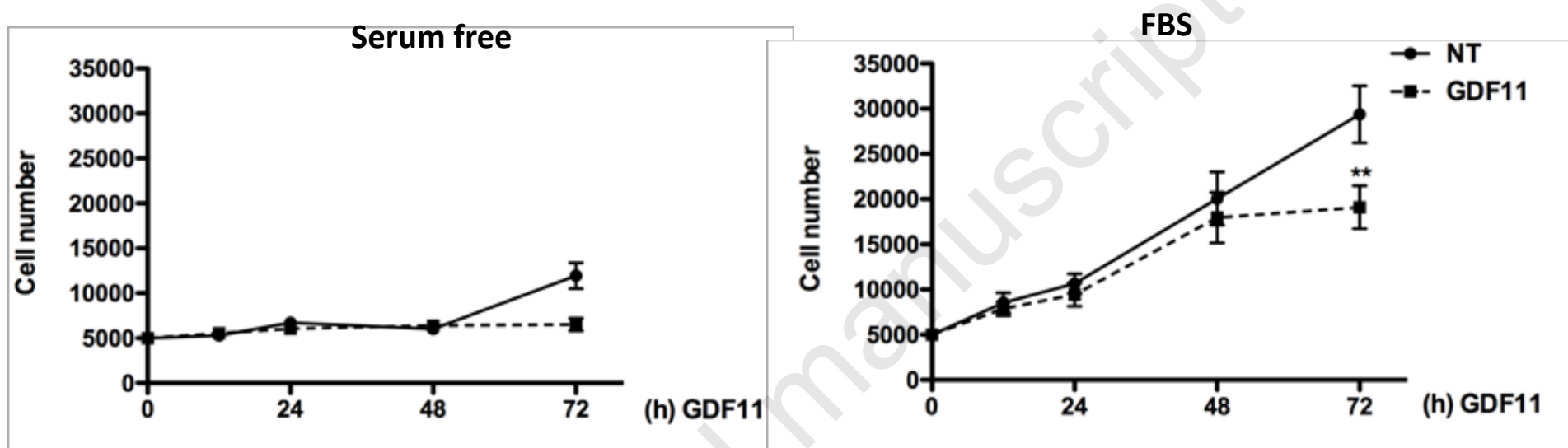
C)



Accepted Manuscript

Figure 2

D)



F)

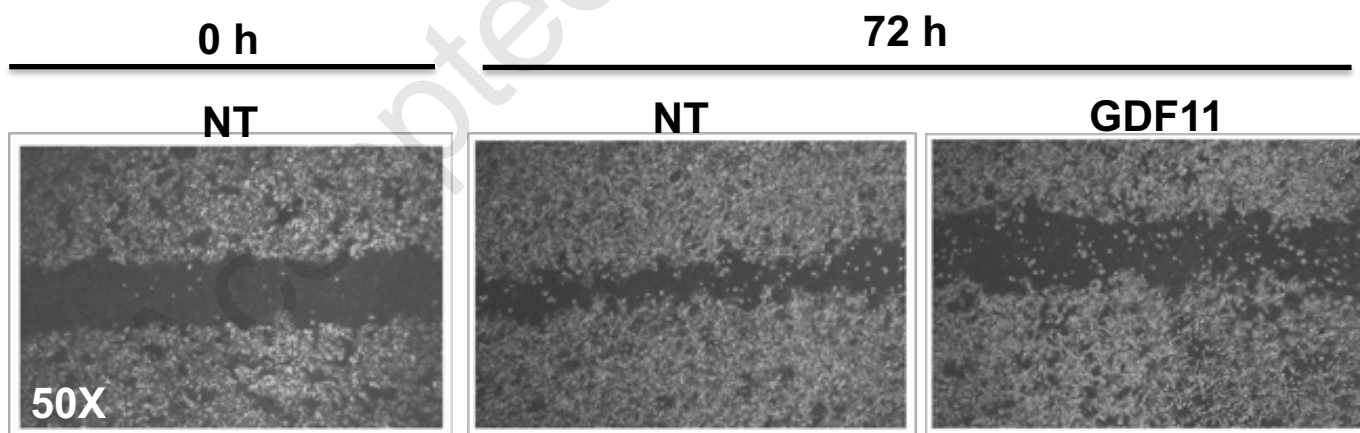
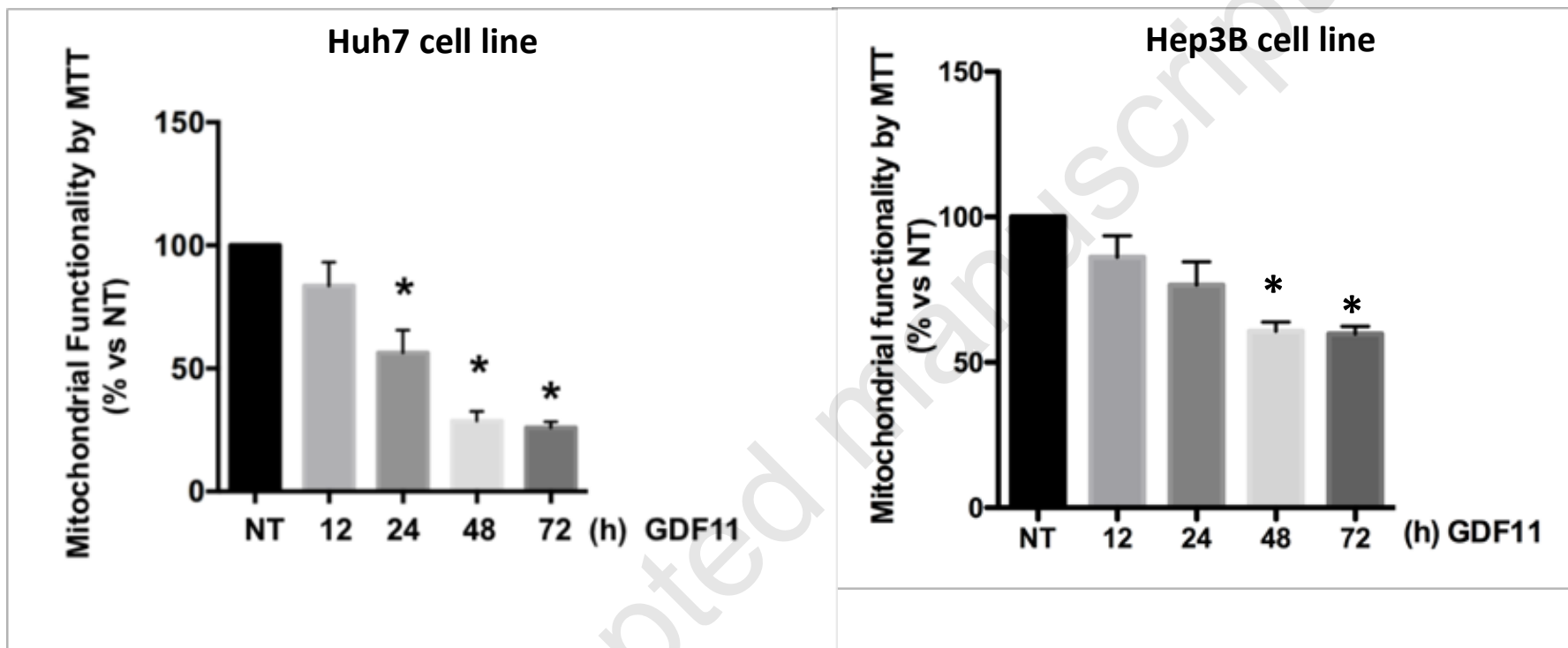


Figure 2

G)



A)

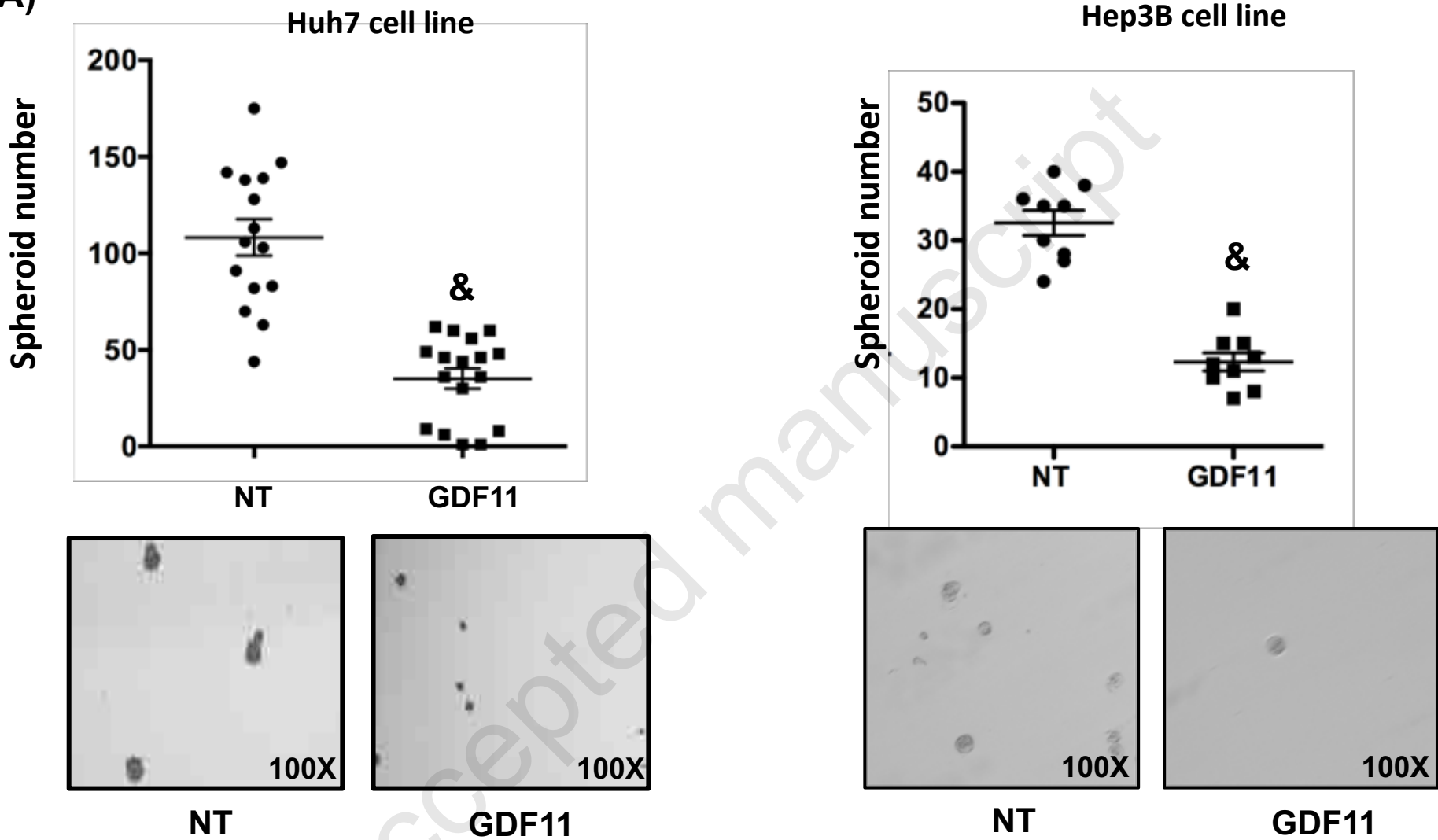
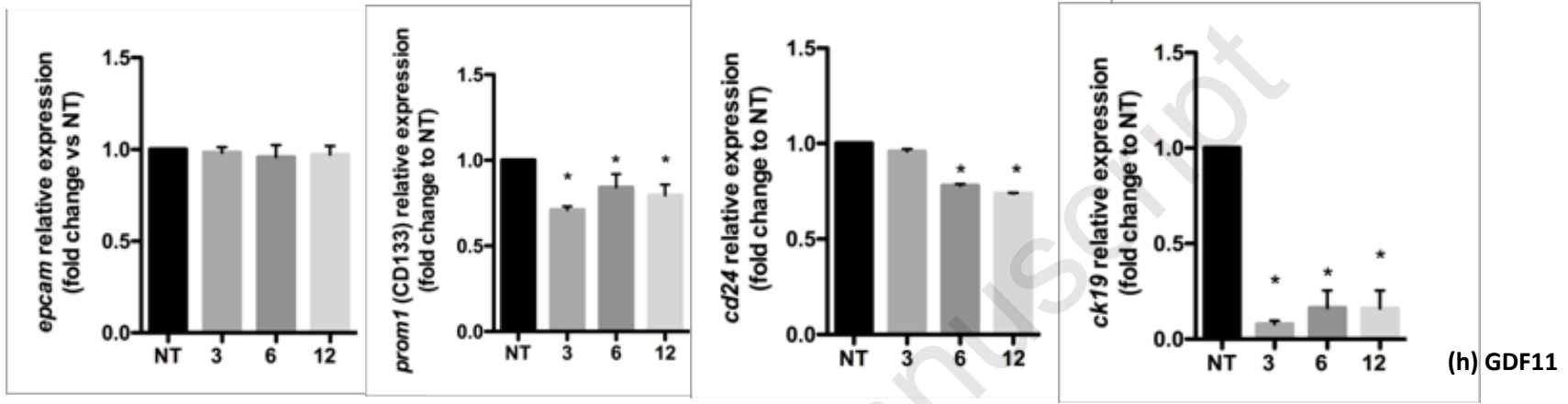


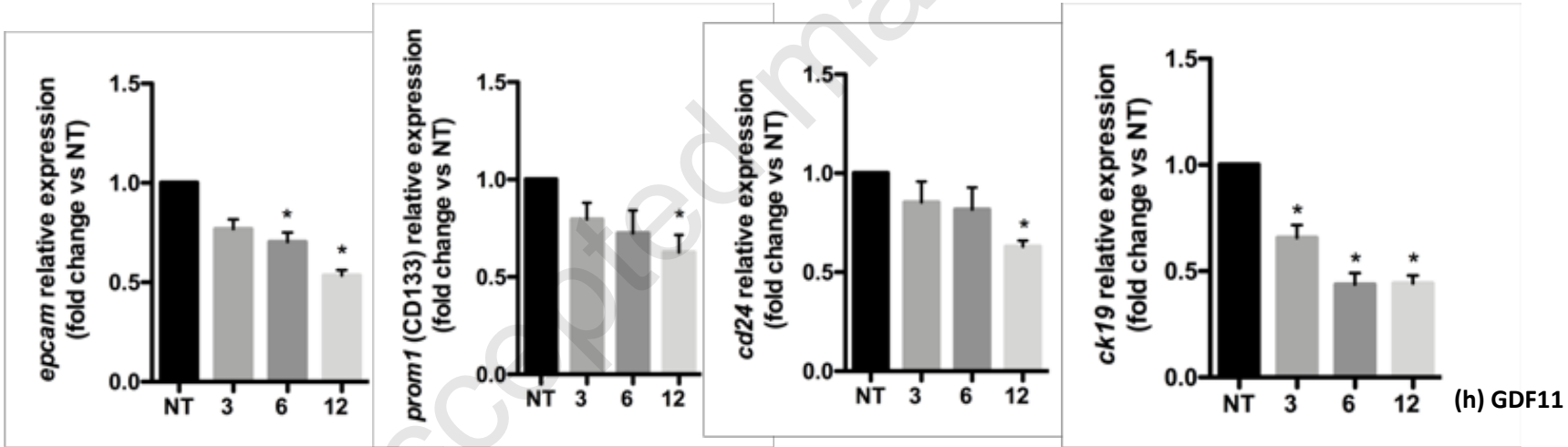
Figure 3

B)

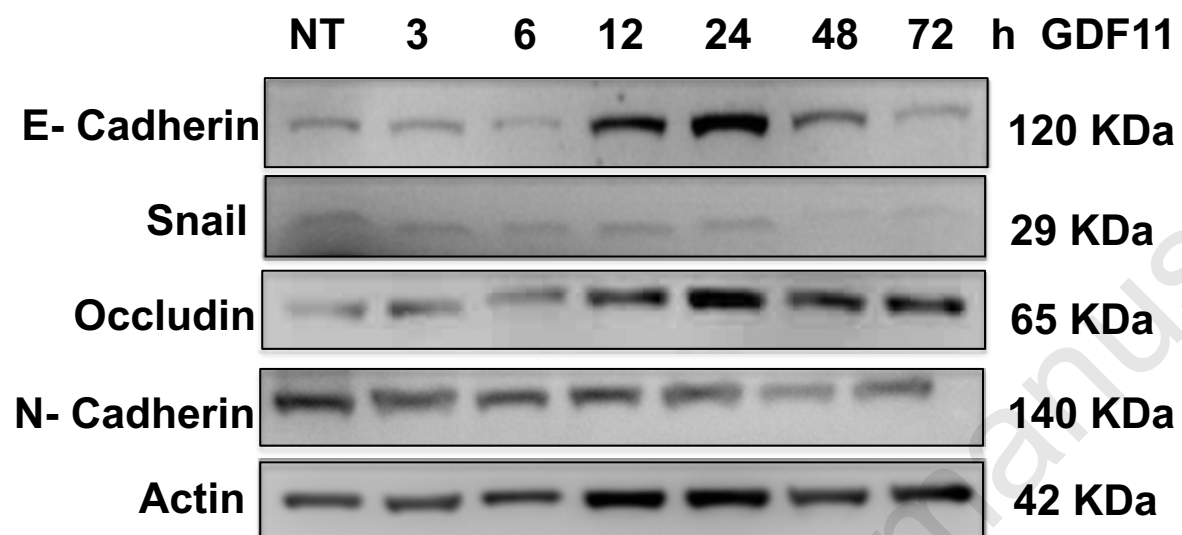
Huh7 cell line



Hep3B cell line



A)



Accepted Manuscript

Figure 4

B)

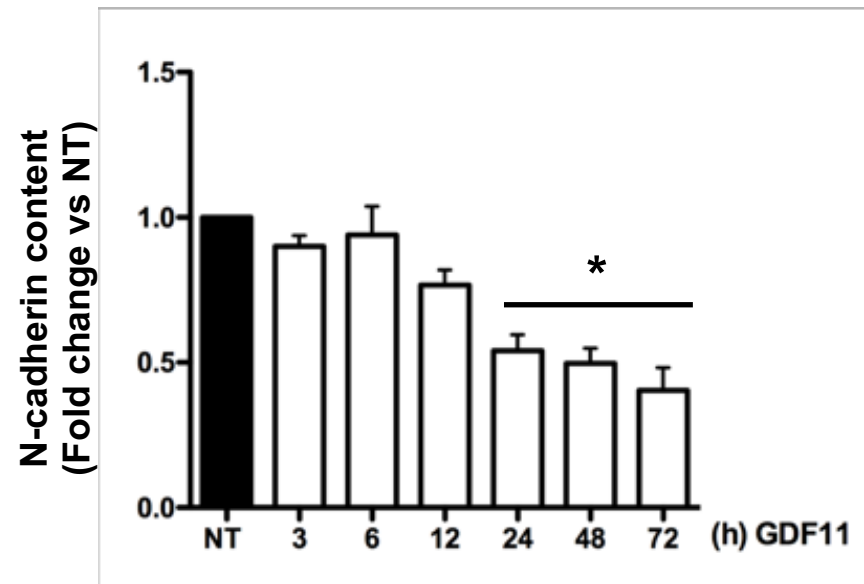
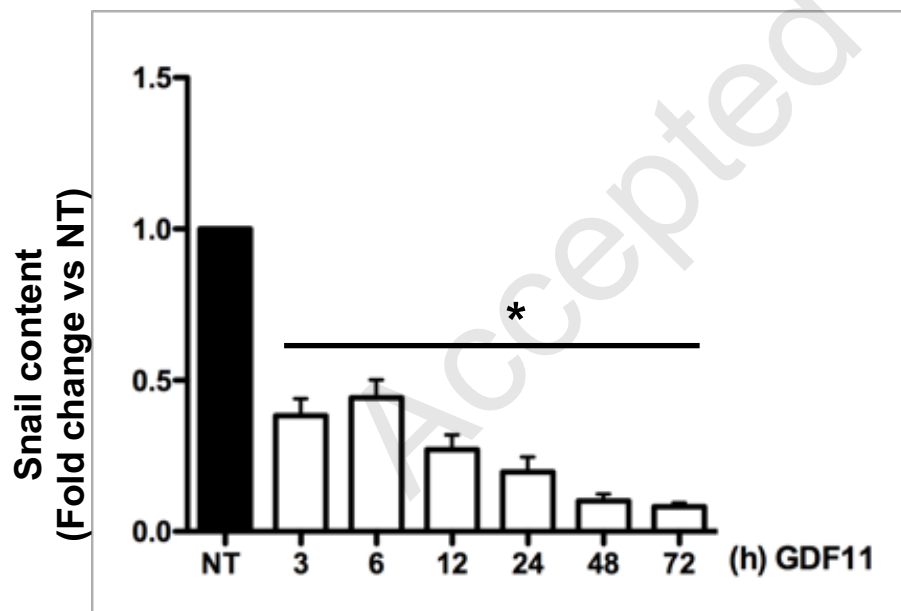
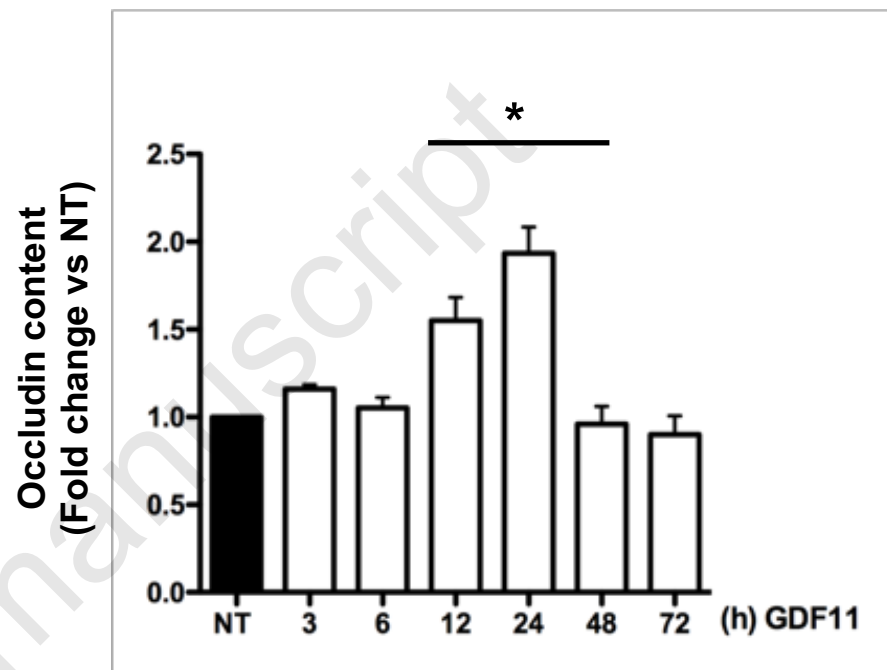
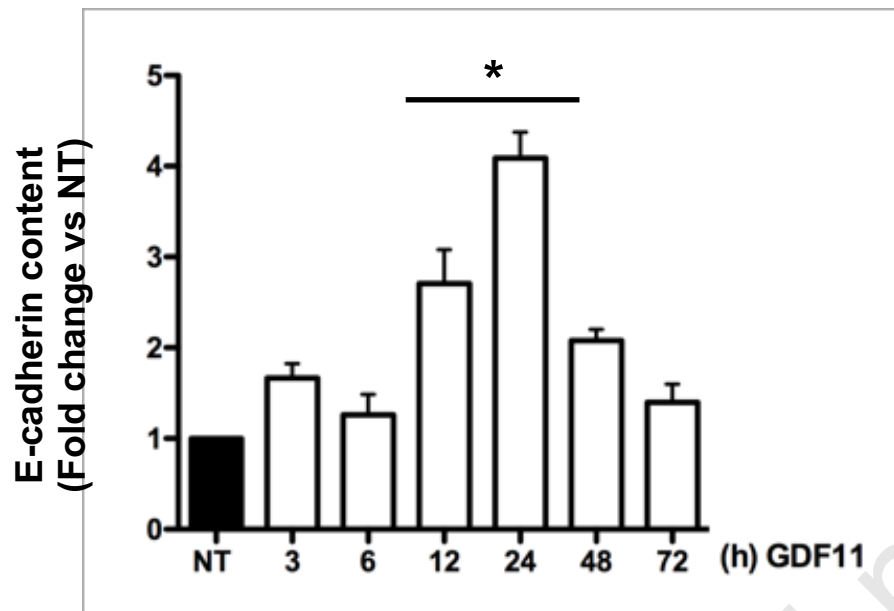


Figure 4

C)

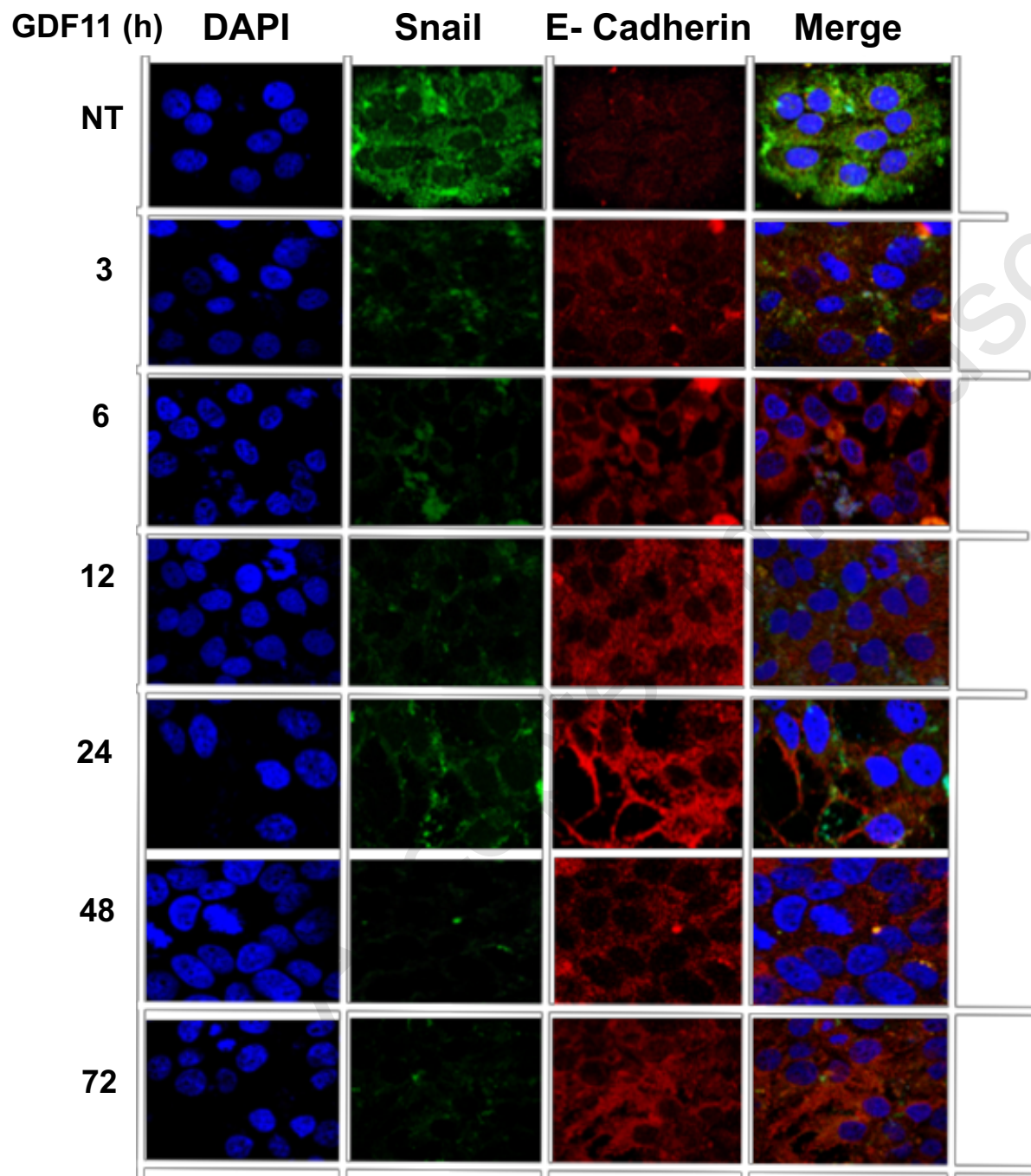


Figure 4

D)

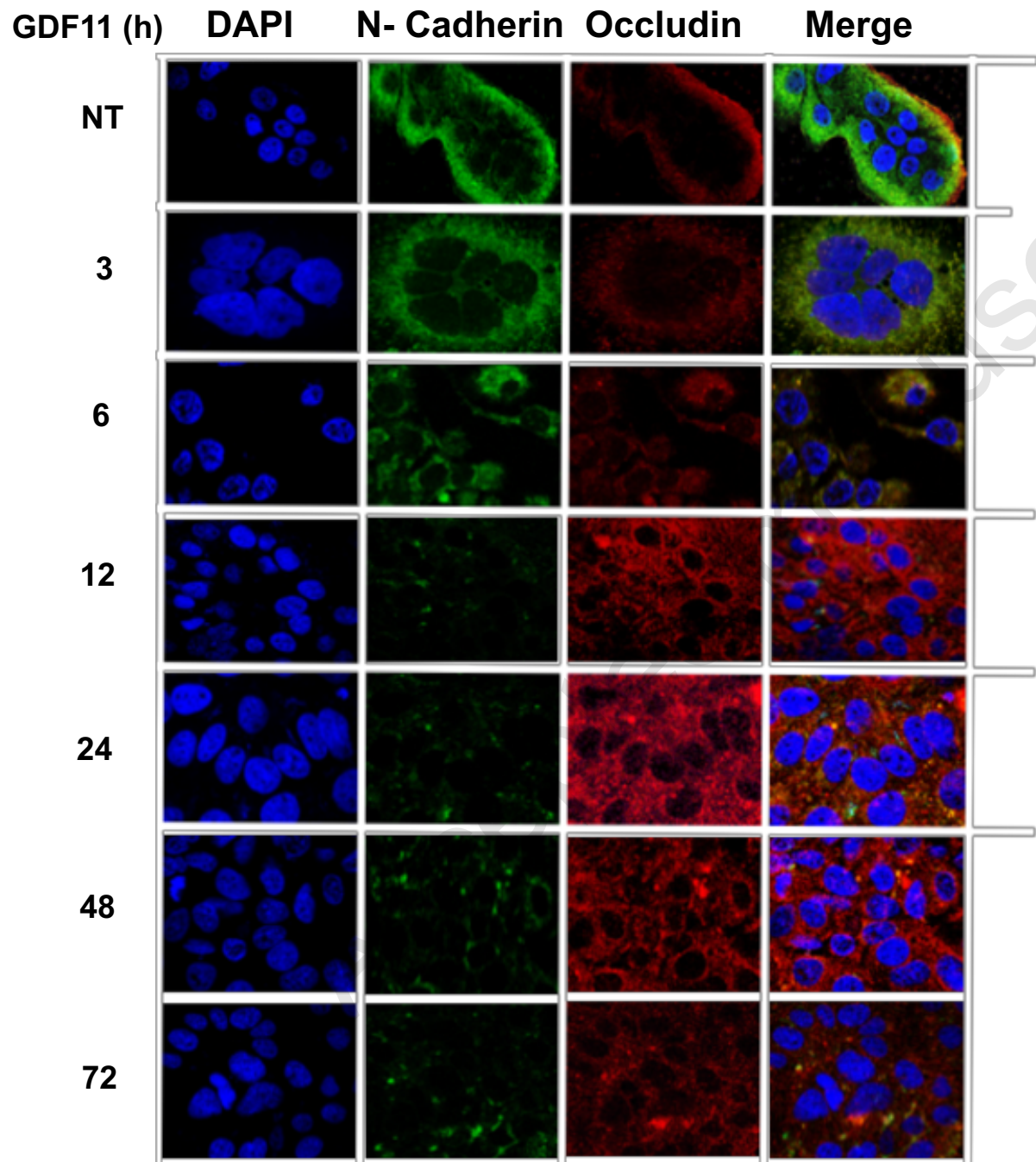


Figure 4

A)

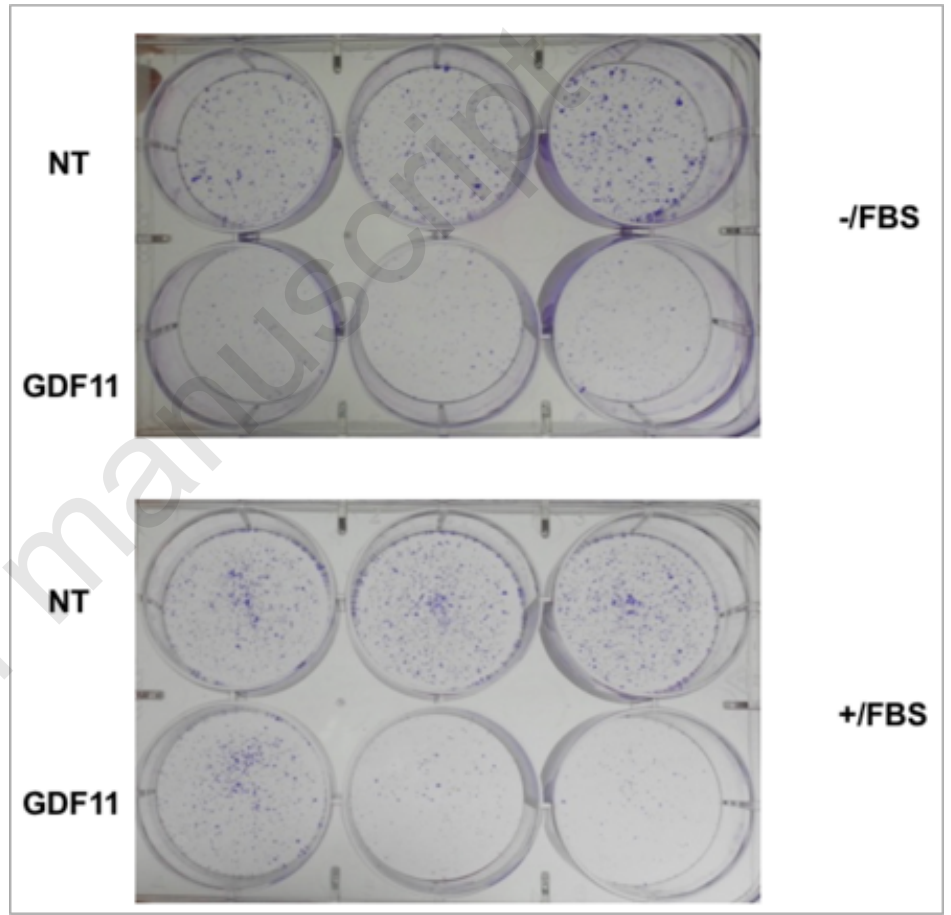
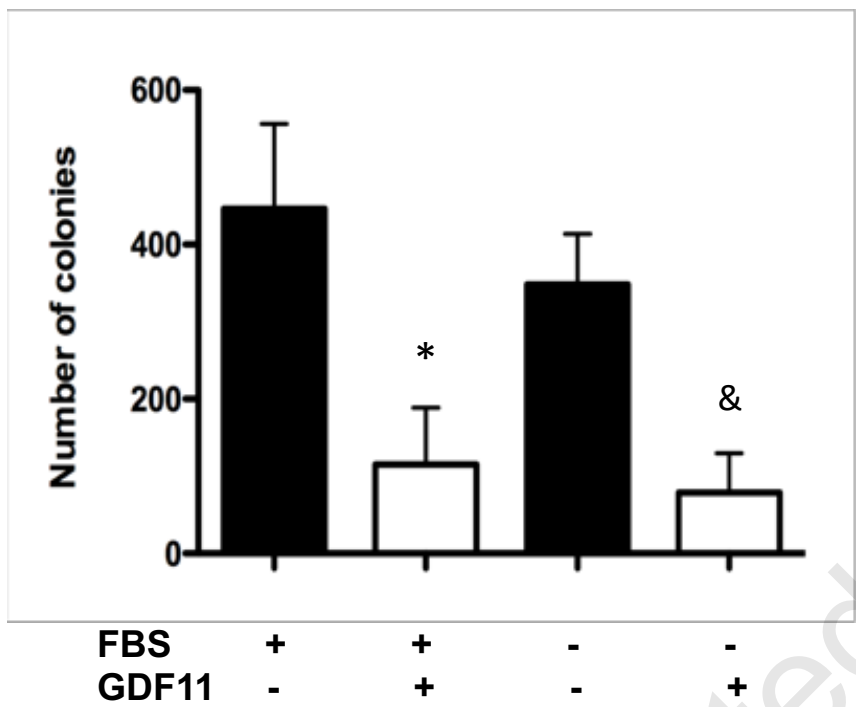
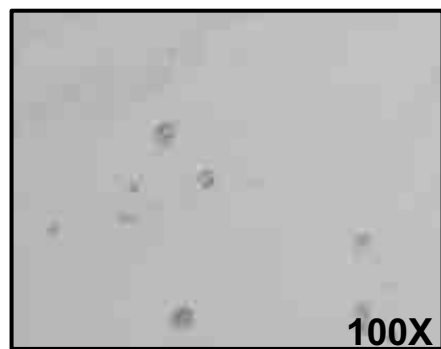
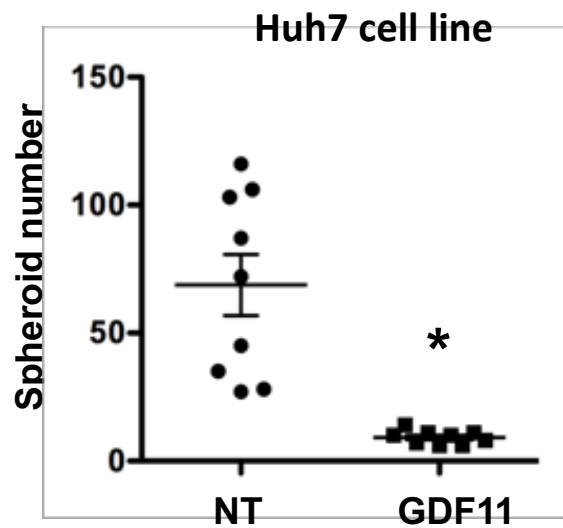
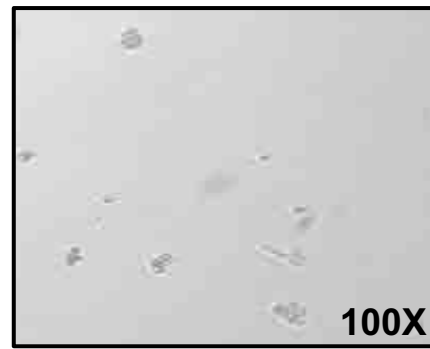
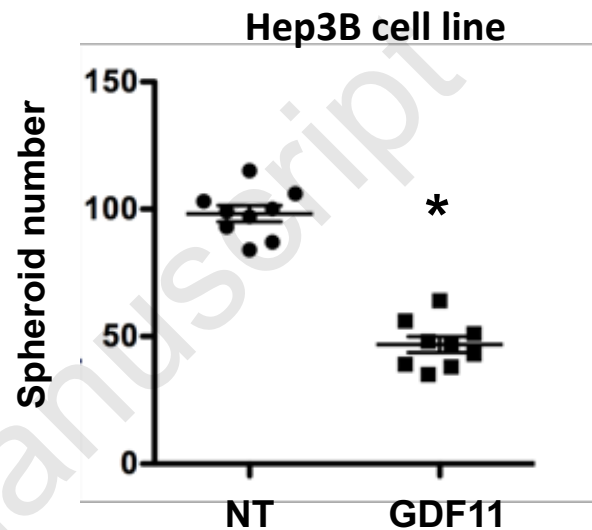
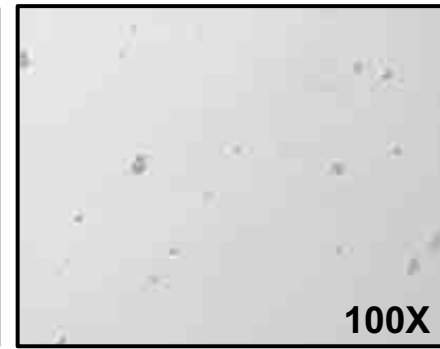


Figure 5

**B)****NT****GDF11****C)****NT****GDF11****Figure 5**

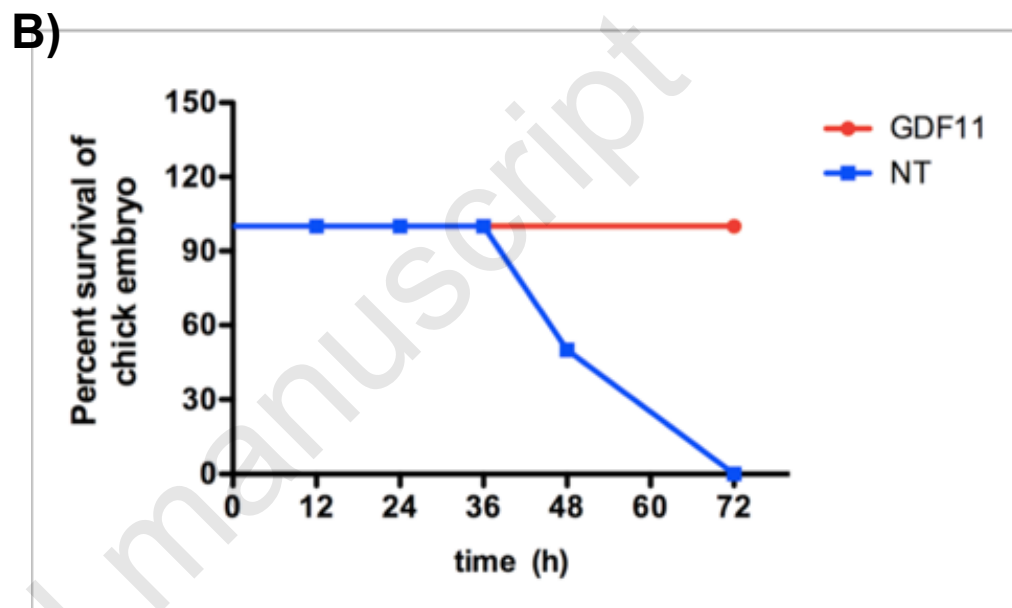
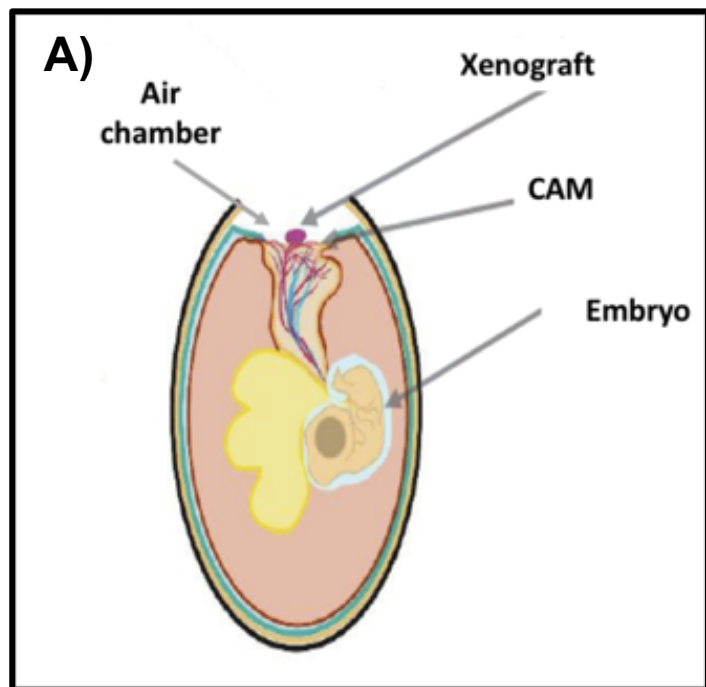
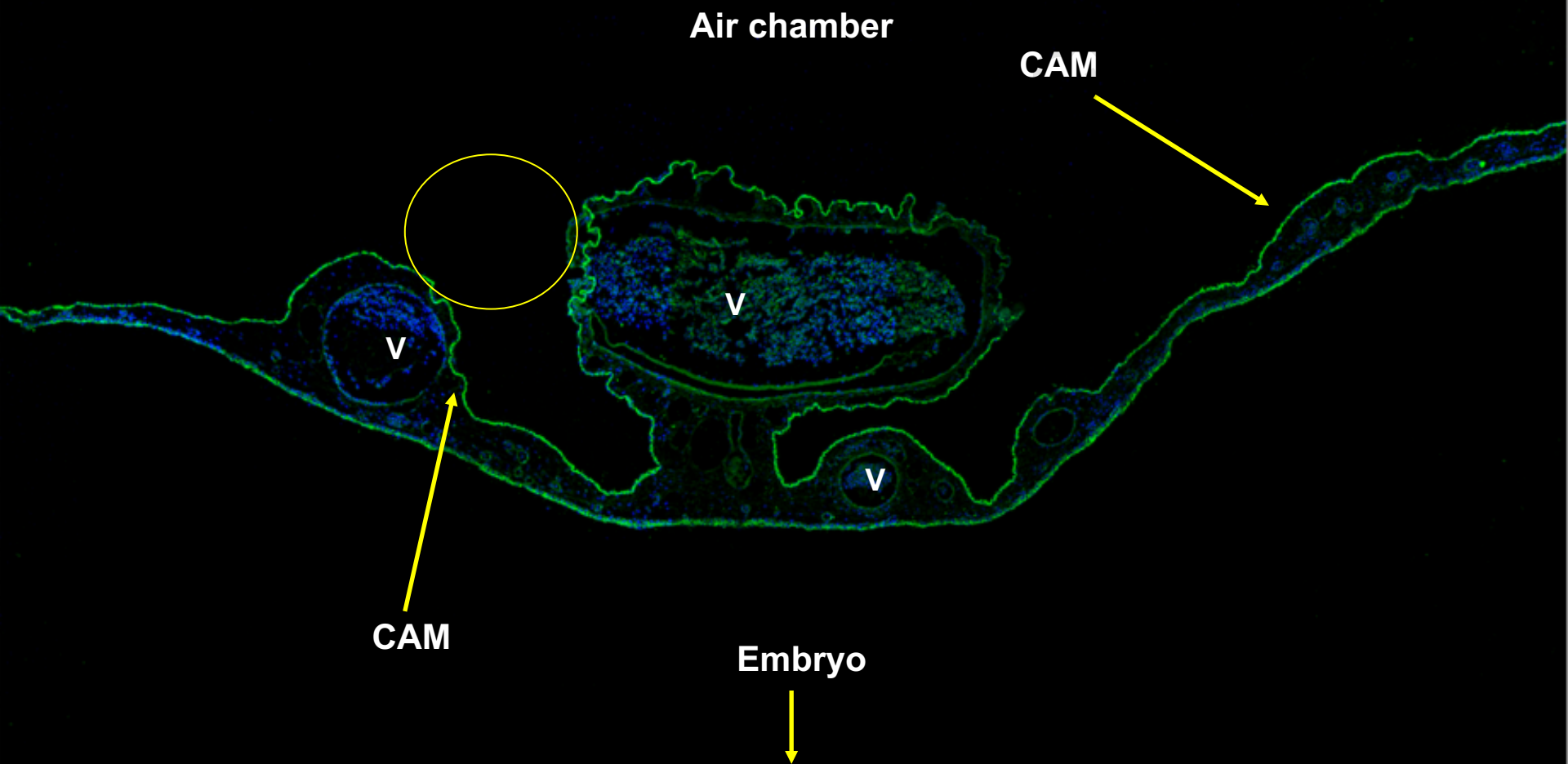


Figure 6

c)

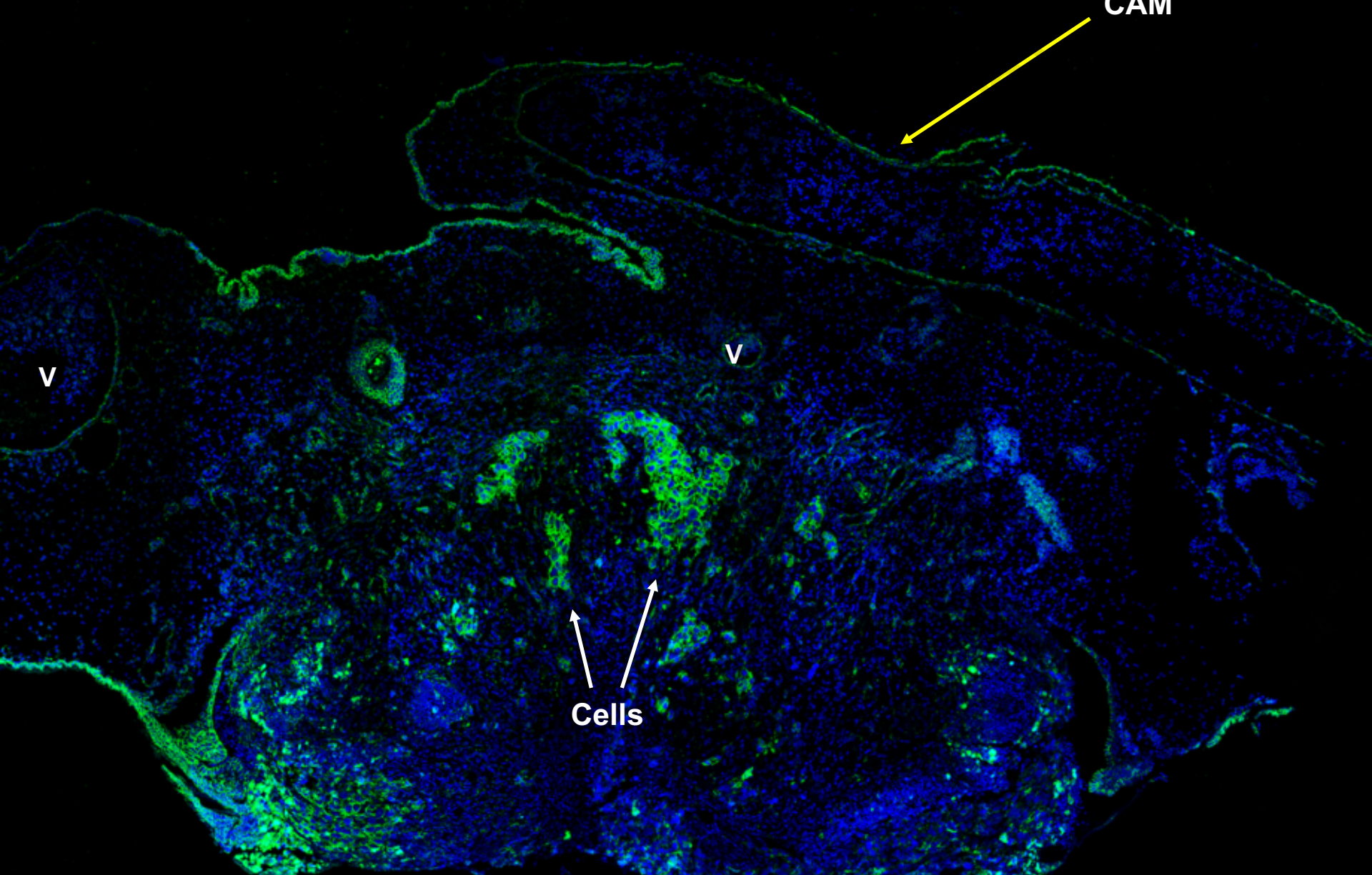


100 μm

**D)**

**Air chamber**

**CAM**



**V**

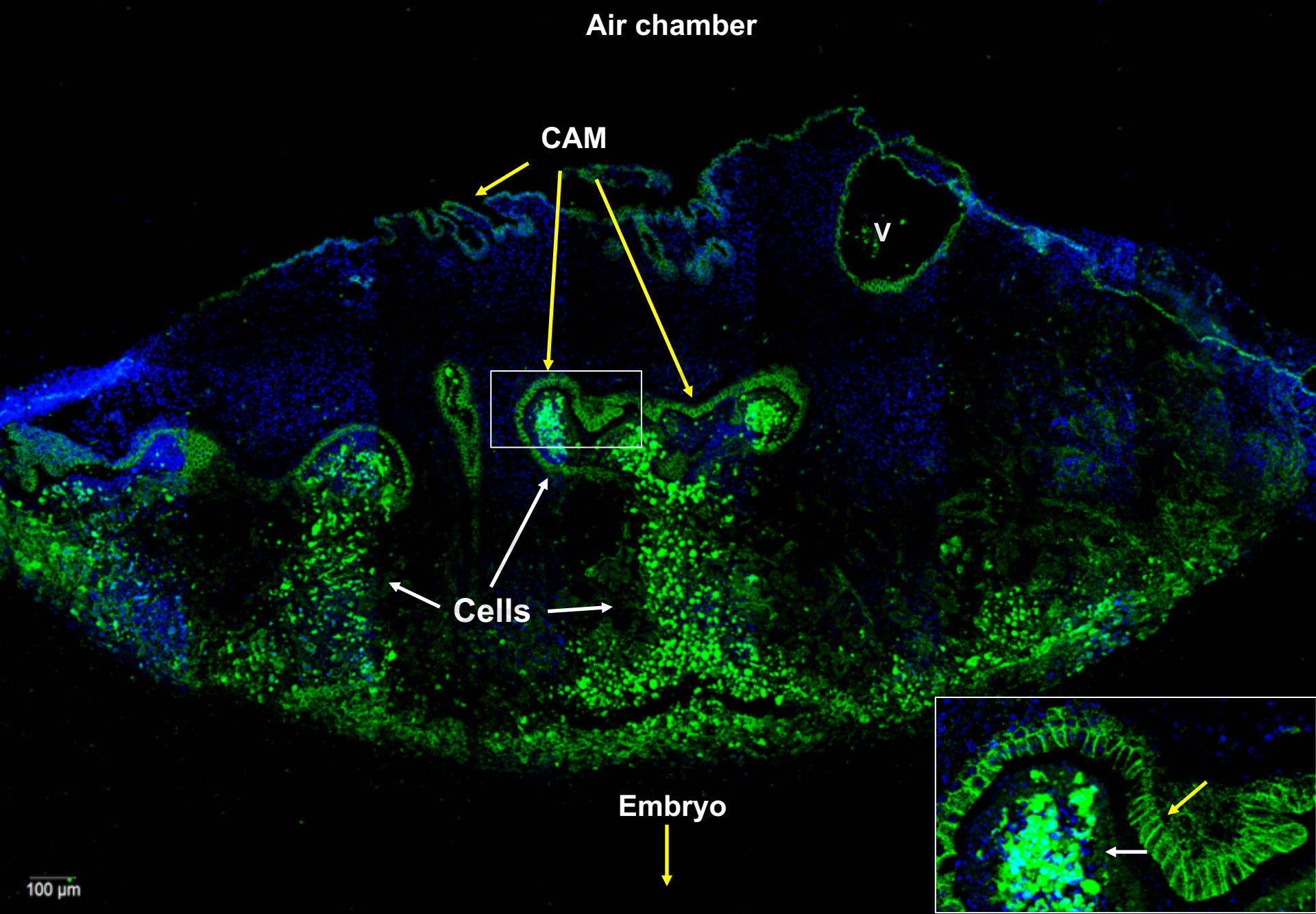
**V**

**Cells**

**Embryo**

100  $\mu$ m

E)



F)

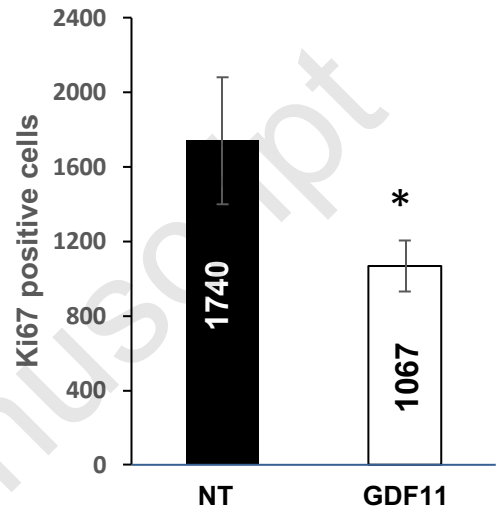
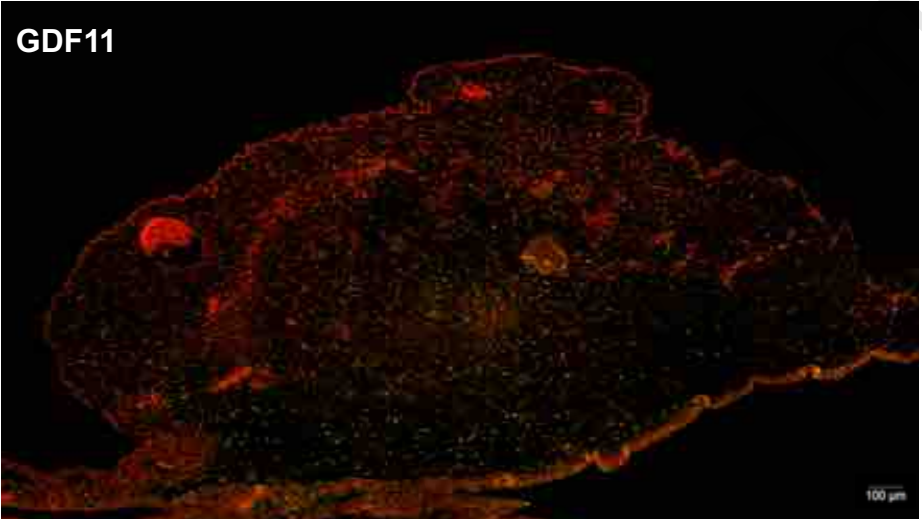
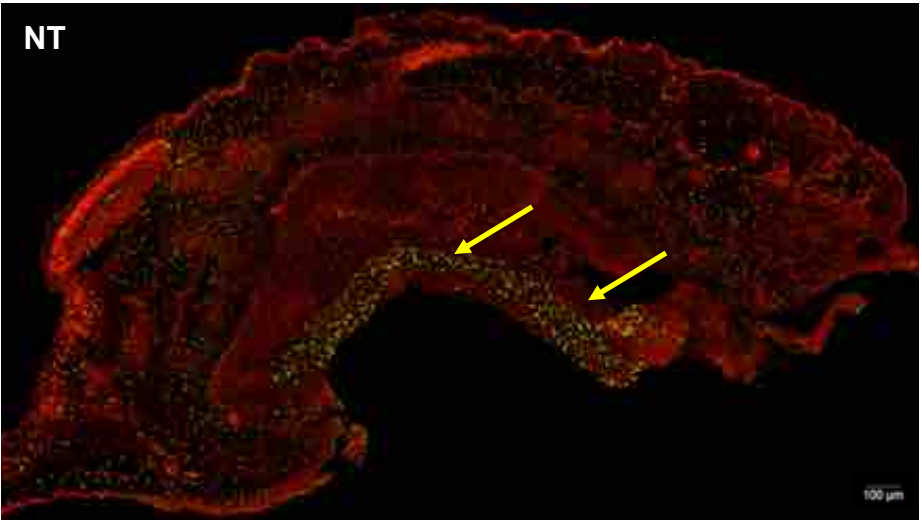
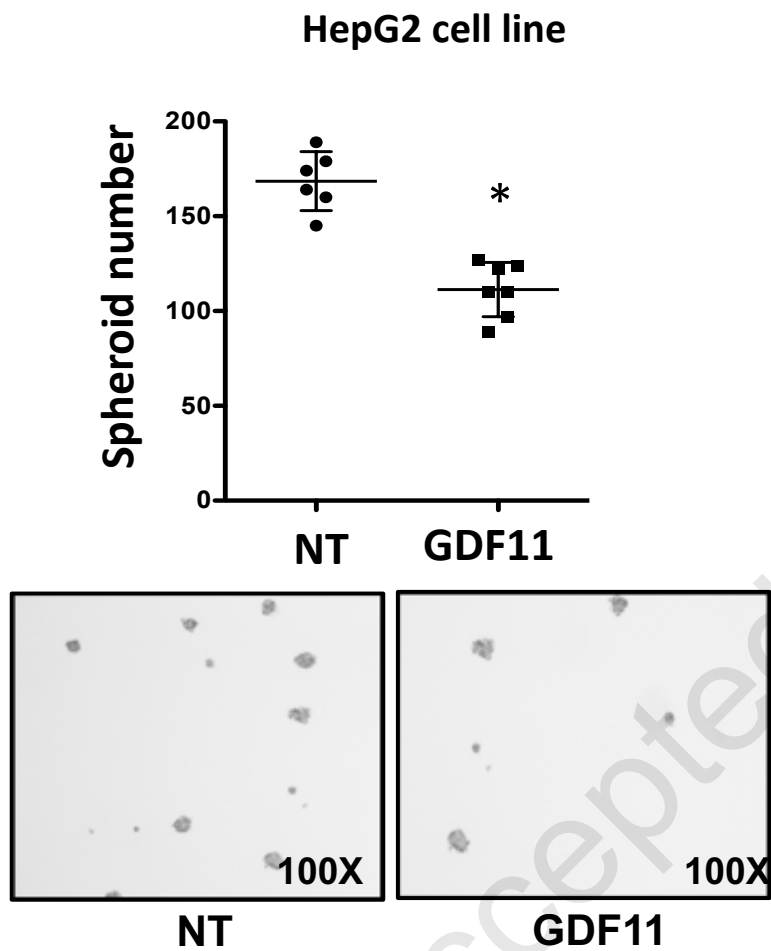
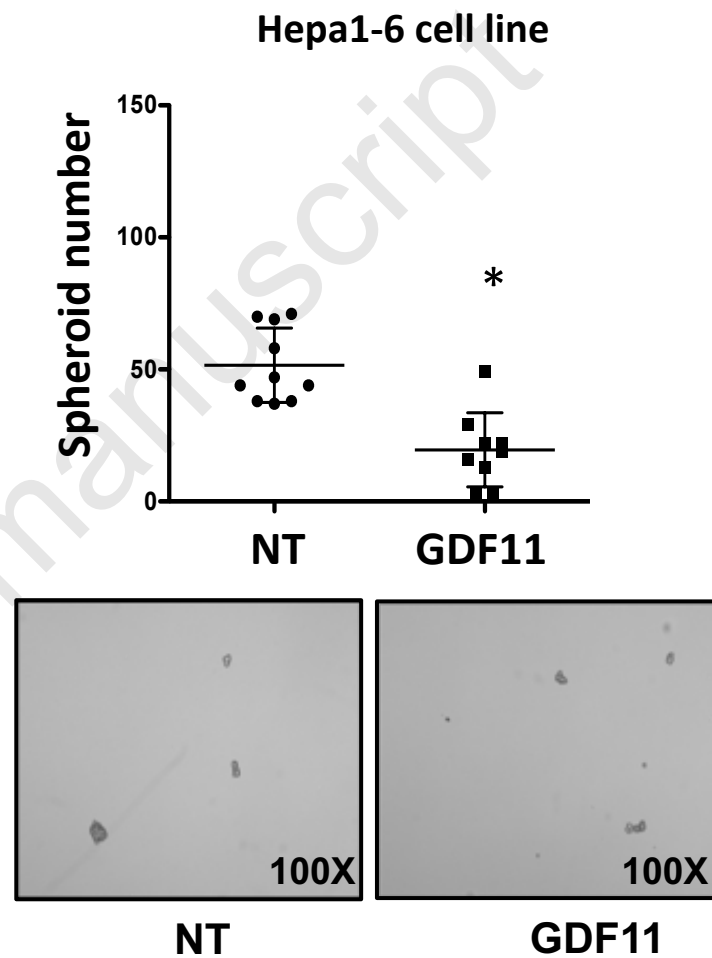
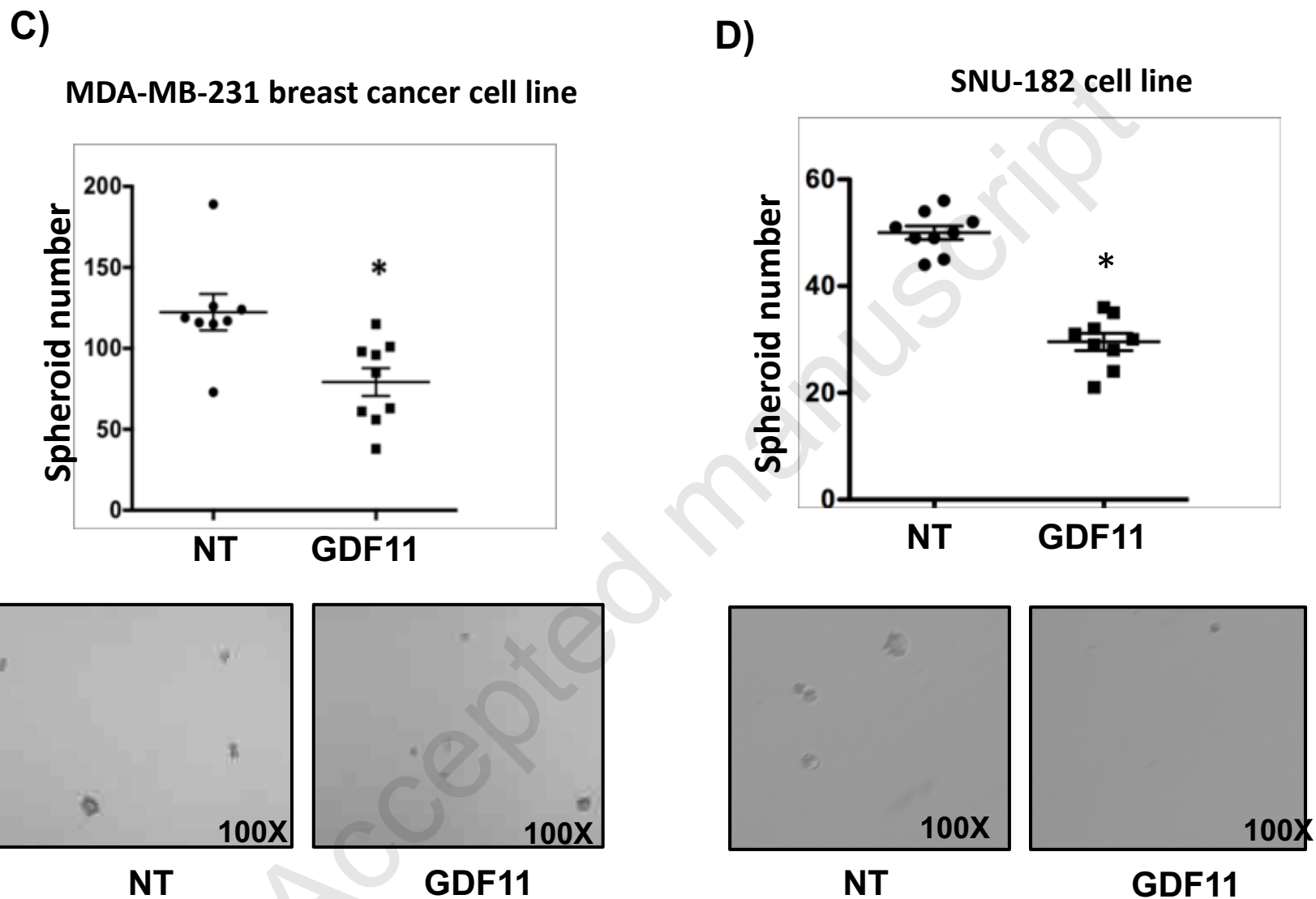


Figure 6

**A)****B)****Figure 7**



**Figure 7**